Engineering a Remarkably Low HOMO – LUMO Gap by Covalent Linkage of a Strong π-Donor and a π-Acceptor—Tetrathiafulvalene-σ-Polynitrofluorene Diads: Their Amphoteric Redox Behavior, Electron Transfer and Spectroscopic Properties

Dmitrii F. Perepichka,[a] Martin R. Bryce,*[a] Andrei S. Batsanov,[a] Eric J. L. McInnes,[b] Jing P. Zhao,[b] and Robert D. Farley[c]

Abstract: Novel $R_3TTF-\sigma-A$ compounds **14**, **16** and **19** (R_3TTF = trialkyltetrathiafulvalene, σ = saturated spacer, A = polynitrofluoren-9-dicyanomethylene acceptor) incorporating very strong donor and acceptor moieties have been synthesized by condensation of the corresponding $R_3TTF-\sigma$-fluoren-9-one diads with malononitrile. Reversible five-step amphoteric redox behavior has been observed with an extremely low HOMO – LUMO gap ($\approx$0.3 eV). For compound **14** a strong EPR signal is observed in the solid state, ascribed to intermolecular complexation: a less intense signal is seen in solution, corresponding to ca. 2% of the molecules existing in a radical form at room temperature. Intramolecular charge transfer in diads **14** and **16** is manifested in strong absorption bands in the near-IR region of their electronic spectra. Spectroelectrochemical data reveal marked electrochromic behavior in the visible and near-IR region of both compounds. The first X-ray crystal structure of a fluorene radical-anion salt is reported, namely the copper salt of 2,4,5,7-tetranitro-9-dicyanomethylenefluorene (1:1 stoichiometry).

Keywords: donor – acceptor systems · electrochromism · electron transfer · HOMO – LUMO gap · tetrathiafulvalene

Introduction

There is continuing interest in low band gap organic materials due to the advanced electronic and electrooptic properties which they display.[1] The main principles for constructing low band-gap polymers include tailoring the aromatic/quinoid character of a conjugated system, its rigidification into a planar conformation, and the alternation of π-donor and π-acceptor fragments in the polymer chain. However, much less is known about monomeric organic compounds with a low HOMO – LUMO gap, which can be engineered by linkage of an electron donor (introducing a high-lying HOMO) and an electron acceptor (introducing a low-lying LUMO) by a spacer unit which precludes mixing of HOMO and LUMO orbitals. These systems represent novel charge transfer materials with predefined D/A stoichiometries for molecular electronics applications, e.g. molecular conductors[2] and molecular switches.[3] This type of molecule, specifically a TTF – σ-TCNQ diad (TTF is tetrathiafulvalene; TCNQ is 7,7′,8,8′-tetracyano-*p*-quinodimethane) was proposed by Aviram and Ratner as a candidate for unimolecular rectification.[4] Since then, TTF derivatives bearing an electron acceptor substituent have been prime targets.[5] Different acceptor groups have been covalently attached to TTF: namely fullerene,[5a–c] phthalocyanines,[5a] pyromellitic diimide,[5d,e] quinones,[5a,f,g] 11,11,12,12-tetracyano-9,10-anthraquinodimethane (TCNAQ),[5a] thioindigo,[5h] viologen and related acceptors,[3a, 5a,d] but these possess only moderate electron affinity (EA). TTFs linked to a strong electron acceptor moiety (i.e., of similar EA to TCNQ) are very difficult to obtain.[6] The only example[6a] of coupling TTF with a substituted TCNQ

[a] Prof. Dr. M. R. Bryce, Dr. D. F. Perepichka, Dr. A. S. Batsanov
Department of Chemistry, University of Durham
Durham DH1 3LE (UK)
Fax: (+44) 191-384-4737
E-mail: m.r.bryce@durham.ac.uk

[b] Dr. E. J. L. McInnes, Dr. J. P. Zhao
EPSRC c.w. EPR Service Centre, Department of Chemistry
The University of Manchester, Manchester M13 9PL (UK)
E-mail: eric.mcinnes@man.ac.uk

[c] Dr. R. D. Farley
EPSRC ENDOR Service Centre, Department of Chemistry
Cardiff University, Cardiff CF10 3TB (UK)
E-mail: rdfarley@cf.ac.uk

Supporting information for this article is available on the WWW under http://www.chemeurj.org or from the author: Experimental details of the preparation of the TTF analogues of **13a** and **13b** and of the reaction of $TTFCH_2OH$ with **17**; ^1H NMR spectra of compounds **5b**, **6**, **18**, **19** and a mixture of **6** + **11**; COSY NMR spectra of compounds **9** and **15**; spectroelectrochemical data for compounds **3b**, **6** and **11**; UV/Vis-near-IR spectrum of **24**; an ORTEP diagram for **18** and a diagram of the disorder in **25** (from X-ray data).

© 2002 WILEY-VCH Verlag GmbH & Co. KGaA, Weinheim
0947-6539/02/0820-4656 $ 20.00+.50/0

(which required an eight-step synthesis) gave EPR-active products, which were difficult to purify and they were not investigated in detail. While many TTF–benzoquinone diads have been reported,[5a,f,g] all attempts to increase their acceptor ability by conversion to the corresponding TCNQ or *N*,*N*′-dicyanoquinodiimine derivatives have failed due to the incompatibility of TTF with the strongly acidic conditions ($TiCl_4$) of these reactions. On the other hand, it is known that condensation of polynitrofluoren-9-ones with malononitrile takes place under milder conditions[7] and the resulting dicyanomethylene derivatives have similar electron affinity to TCNQ. With this in mind we now report[8] the first TTF–fluorene conjugates which posses both strong electron donor and strong acceptor properties.

Results and Discussion

Synthesis: The covalent linkage of a TTF fragment to a fluorene acceptor was first achieved through the formation of an ester or amide bond. Contrary to the previously used methodology for TTF–σ–TCNAQ diads,[9] the carbonyl group was placed on the acceptor (fluorene) component, because when attached to the TTF system, it raises its oxidation potential. The synthesis of the fluorene carbonyl chlorides **5a**,**b** with different length σ-bridges is presented in Scheme 1.

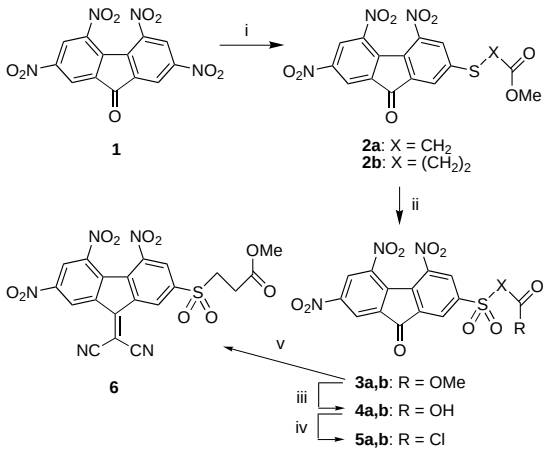

Scheme 1. i) HS-X-CO_2Me+$NaHCO_3$/MeCN, 20 °C, 2–6 h; ii) H_2O_2/AcOH, 60–70 °C, 3 h; iii) CF_3CO_2H/H_2O, reflux, 4–6 h; iv) $(COCl)_2$/CH_2Cl_2, 20 °C, 20–40 h; v) $CH_2(CN)_2$/DMF, 20 °C, 6 h.

The 2-nitrogroup in compound **1** was selectively substituted with 2-mercaptoacetic or 3-mercaptopropionic ester in acetonitrile solution in the presence of $NaHCO_3$ (as a base catalyst and as a trap for the nitronic acid formed during the reaction). These conditions were superior to those described earlier for butylmetcaptan where aprotic dipolar solvents and no catalyst were used.[10] The resulting sulfides **2a**,**b** were oxidized to sulfones **3a**,**b** with hydrogen peroxide in acetic acid and the ester group was then converted to the acids **4a**,**b** and acid chlorides **5a**,**b** by treatment with aqueous trifluoroacetic acid and oxalyl chloride, respectively. The overall yield for the four steps was 33% and 72% for **5a** and **5b**, respectively.

The donor synthons were obtained from TTF derivative **7**[9] containing alkyl substituents to lower the oxidation potential and pentyl chains to improve solubility, as shown in Scheme 2.

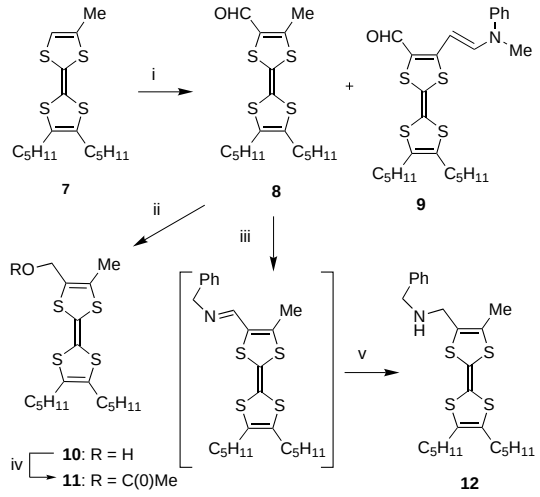

Scheme 2. i) LDA/Et_2O, −78 °C, 2 h, then PhN(Me)CHO −78 °C → 20 °C, 12 h; ii) $NaBH_4$/EtOH, 20 °C, 1 h; iii) $PhCH_2NH_2$ + 4 Å MS/cyclohexane, reflux, 15 h; iv) PhCOCl + Py/MeCN, 20 °C, 2 h; v) $LiAlH_4/Et_2O$, 20 °C, 3.5 h.

The reaction of the lithium salt of **7** with *N*-methylformanilide afforded aldehyde **8** (66% yield) together with compound **9** (5% yield) as a product of a base-catalyzed condensation of **8** with a second molecule of *N*-methylformanilide. Aldehyde **8** was reduced with $NaBH_4$ to give hydroxymethyl-TTF **10**. The synthesis of aminomethyl-TTF by amination of (unsubstituted) TTF-carbaldehyde followed by reduction of the Schiff base has been reported and the best yield (35%) was achieved for the *N*-benzyl derivative.[11] A slightly modified procedure in our case gave a significantly higher yield of amine **12** (88% from **8**) which might be a useful synthon for the incorporation of a TTF moiety into other systems.

The TTF–fluorene conjugates (Scheme 3) were synthesized by coupling of the acid chlorides **5a**,**b** with the alcohol **10** using pyridine as a nucleophilic catalyst (basic catalysis, e.g. Et_3N, is not applicable due to the high sensitivity of polynitrofluorenes to bases). Alternatively, diad **13b** was synthesized by direct esterification of acid **4b** with alcohol **10** using dicyclohexylcarbodiimide and *p*-(dimethylamino)pyridine catalysis. The ester bond in compounds **13a**,**b** and **14** under certain conditions might be sensitive to hydrolysis; therefore, the amide derivatives **15** and **16** were synthesized from amine **12**.

The D–σ–A diads **13**–**16** possess flexible σ-bridges which are long enough to allow intramolecular π–π complexation (see below). Using fluorene-4-carbonyl chloride derivative **17** as an acceptor synthon would provide a shorter σ-bridge precluding the formation of an intramolecular complex. However, in a model reaction, attempted coupling of acid chloride **17** with $TTFCH_2OH$ under the conditions used for **5** (pyridine catalysis) did not afford the target diad. Instead, the radical cation salt $(TTFCH_2OH^{+\bullet})Cl^-$ was isolated in 90% yield, probably as the result of an electron transfer reaction

 © 2002 WILEY-VCH Verlag GmbH & Co. KGaA, Weinheim 0947-6539/02/0820-4657 $ 20.00+.50/0

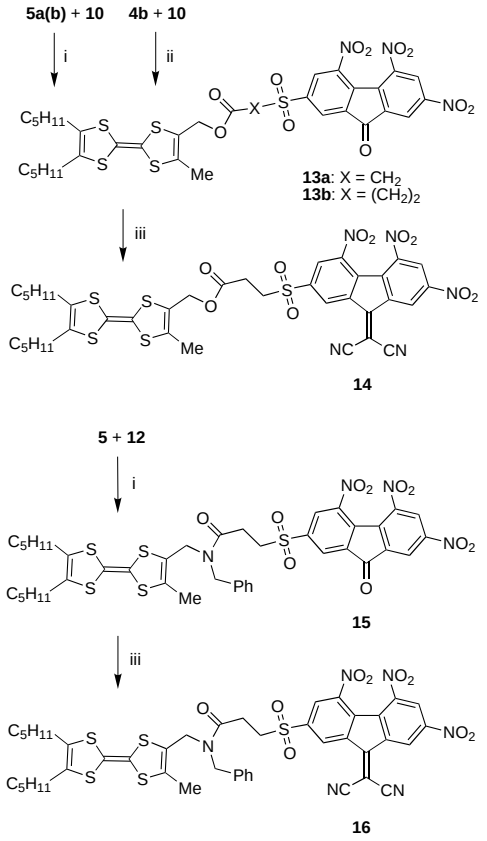

Scheme 3. i) Pyridine/MeCN, 20 °C, 6 h; ii) dicyclohexylcarbodiimide + 4-dimethylaminopyridine/CH_2Cl_2, 20 °C, 15 h; iii) $CH_2(CN)_2$/DMF, 20 °C, 6 h.

between the TTF-methanol and a strongly electron accepting intermediate, such as 2,5,7-trinitrofluorene-9-one-4-carbonyl-*N*-pyridinium. Compound **10** similarly gave a cation radical salt. Diad **18** was, however, synthesized in 78% yield by coupling of the acid chloride **17** with the lithium alkoxide derivative of **10** at −100 °C. The electron transfer reaction also did not occur when a milder acceptor was employed, namely the acid chloride **20** for which the pyridine-catalyzed reaction with $TTFCH_2OH$ gave D–σ–A diad **21** in 86% yield (Scheme 4).

The acceptor ability of the fluorene moiety in **13b**, **15** and **18** was increased by conversion to the dicyanomethylene derivatives **14**, **16** and **19**, respectively, by treatment with malononitrile in DMF solution (Schemes 3 and 4). As the separation of the dicyanomethylene derivatives from the starting fluorenones was difficult, a large excess of malononitrile was employed to complete the conversion. Under these conditions a deep-blue by-product was obtained, the yield of which increased in the presence of silica gel.[12] To elucidate its structure, the reaction between fluorenone **1** and the excess of malononitrile was performed in DMF and DMSO (the reaction goes faster in DMSO) in the presence of silica gel. A second molecule of malononitrile substitutes the cyano group[13] in the initially formed 9-dicyanomethylenefluorene (**22**) to give a tricyanovinyl derivative which being an exceptionally strong C-H acid exists in its carbanion form **23** (Scheme 5); the structure of **23** was established by X-ray analysis of a potassium complex. The source of potassium is believed to be potassium salts present in the silica gel.[14]

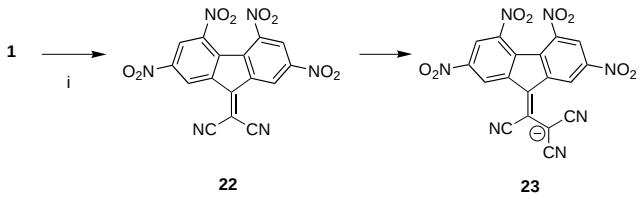

Scheme 5. i) $CH_2(CN)_2$, SiO_2/DMSO, 20 °C, 12 h.

The anion radical salts of **22** were synthesized as model compounds with complete charge transfer. Lithium and copper salts **24** and **25** were prepared by the electron transfer reaction of **22** with lithium iodide and copper wire, respectively, and a single crystal of **25**·MeCN was grown for X-ray analysis.

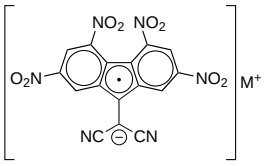

IR Spectra: The high sensitivity of the nitrile stretching frequency to the charge accumu-

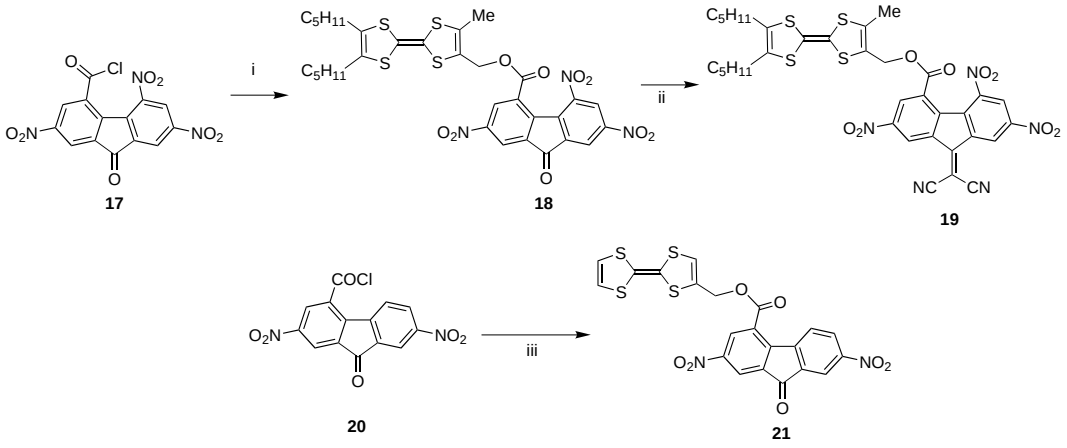

Scheme 4. i) **10** + BuLi, THF, −100 °C → 20 °C, 1 h, then + **17**, −100 °C → −15 °C, 3 h, then −15 °C, 12 h; ii) $CH_2(CN)_2$/DMF, 20 °C, 8 h; iii) $TTFCH_2OH$ + pyridine/MeCN, 20 °C, 12 h.

© 2002 WILEY-VCH Verlag GmbH & Co. KGaA, Weinheim
0947-6539/02/0820-4658 $ 20.00+.50/0 *Chem. Eur. J.* **2002**, *8*, No. 20

lated on the molecule can be utilized to monitor charge-transfer interactions involving cyano-substituted acceptors. For example, for TCNQ $\tilde{\nu}_{C\equiv N} = 2225$ and 2180 cm^{-1} for the neutral and anion radical species, respectively.[15] The $\tilde{\nu}_{C\equiv N}$ of the diads **14**, **16** and **19** (ca. 2203 cm^{-1} in KBr pellets[16]) is substantially lower than that of similar fluorene acceptors without a TTF moiety, e.g. **6** and **22** (2235 cm^{-1}). We attribute this to significant charge transfer in the solid state of **14**, **16** and **19**. The value of $\tilde{\nu}_{C\equiv N}$ for the anion radical salt **24** is further lowered to 2185 cm^{-1}[17] and, therefore a degree of CT (δ_{CT}) ≈ 0.65 electrons can be calculated for **14**, **16** and **19**.[18] A similar value of δ_{CT} (0.6–0.7 electrons) could be also predicted[18] from the difference in oxidation and reduction potentials of the donor and acceptor moieties (see the Electrochemistry Section). Only small variations (within 5 cm^{-1}) in the ketone C=O stretching frequency were found in fluorenones **3**, **13**, **15** and **18** in accord with the significantly reduced charge transfer in these diads.

^{1}H NMR spectra: ^{1}H NMR spectra of compounds **14**, **16** and **19** in [D_6]acetone solution feature broadened signals of the protons adjacent to both the TTF and fluorene fragments which indicates a significant spin concentration (see the EPR section) on the D and A moieties (paramagnetic broadening, PMB). The extent of this broadening is inversely proportional to the distance of the resonant group to the radical center (i.e., fluorene or TTF) and it was not observed in diads **13**, **15** and **18** which possess a weaker acceptor moiety. The broader signals of 3-H and 6-H compared with 1-H and 8-H[19] indicate a higher spin concentration in the former positions of the fluorene nuclei.[7] A weaker PMB in acetone solution was previously reported for other strong fluorene acceptors (as a result of interaction with basic impurities)[7] but it is not observed in this solvent for TTF molecules alone. In the case of fluorene acceptors without a TTF substituent the PMB could be completely suppressed by addition of traces of CF_3COOH. For the D–A diads addition of CF_3COOH results in only partial restoration of the resolution of the protons adjacent to fluorene (and further enhances the PMB of protons adjacent to TTF[20]). Pure fluorene **6** (representing the A part of diads **14** and **19**) gave a clear sharp ^{1}H NMR spectrum, but on mixture with the TTF derivative **11** (representing the D part) in [D_6]acetone solution in 4×10^{-2} M concentration, a very similar PMB is observed (see Supporting Information). Based on these data we suggest that PMB for **14**, **16** and **19** is due to electron transfer from the TTF moiety onto the fluorene nucleus.

Another special feature in the NMR spectra resulting from a donor–acceptor interaction is seen for the amide-linked diads **15** and **16**. The known slow rotation around a C(O)–N amide bond results in two sets of signals in a $\approx$1:2 ratio corresponding to the *E* and *Z* isomers (see Figure S2 in Supporting Information). The difference in the chemical shifts of both isomers ($^{E-Z}\Delta\delta$) should normally rapidly decrease with the distance between the amide bond and a resonant group. However, in the case of **15** quite high $^{E-Z}\Delta\delta$ values (0.117 and 0.058 ppm) were found for the fluorene protons in the 1- and 3-positions.[19] This value is close to that of both N-CH_2 groups ($^{E-Z}\Delta\delta = 0.151$ and 0.101 ppm) and even higher than that of SO_2CH_2 ($^{E-Z}\Delta\delta = 0.036$ ppm) and CH_2CON ($^{E-Z}\Delta\delta = 0.040$ ppm) protons (which are much closer to the isomerized bond), but no observable difference in the shift for the isomers ($^{E-Z}\Delta\delta < 0.005$ ppm) was found for 6-H and 8-H protons. This is very unlikely to be a "through-bond" transmitted effect, and we explain it by a contribution of a head-to-tail folded, $\pi-\pi$ intramolecularly complexed conformation of these diads where a "through-space" interaction can take place. The remarkable difference in the behavior of the 1,3-H and 6,8-H protons could be a result of the ICT complex topology where the $\pi-\pi$ interaction occurs mostly between the TTF unit and the sulfonyl substituted benzene ring of the fluorene nuclei. A similar trend was observed for a stronger acceptor **19**: $^{E-Z}\Delta\delta = 0.171$ ppm for 1-H and = 0.01 ppm for 8-H protons (the shifts of 3-H and 6-H protons could not be determined due to PMB effect, Figure S3 in the Supporting Information).

EPR Spectra: The high donor and acceptor ability of the TTF and fluorene moieties, respectively, in **14** results in facile electron transfer in this compound, which is manifested in a strong EPR signal in the solid state and a less intense signal in solution (Figure 1). Dichloromethane and acetone fluid solutions of **14** reveal a broad (2.6 G in CH_2Cl_2 at 298 °C) single line, centered at $g_{iso} = 2.007$ (Figure 1a).[21] Frozen CH_2Cl_2 solutions and powdered samples give rise to a rhombic spectrum with *g* values: $g_1 = 2.014$, $g_2 = 2.006$ and $g_3 = 2.002$ (Figure 1b). The anisotropic *g* values average well to the isotropic value $g_{iso} = 2.007$, and are almost the same as those reported for substituted TTF radical cations.[22] Therefore, we assign these EPR signals to the radical cation of the TTF moiety. However, there is no indication of a second radical species (corresponding to the fluorene radical anion), even at Q-band frequency, although the PMB effect in the NMR spectra suggests significant spin concentration is present on the fluorene moiety. It is possible that this second signal is quenched by formation of head-to-head dimers; a similar process has been observed for the radical anion of TCNQ.[23]

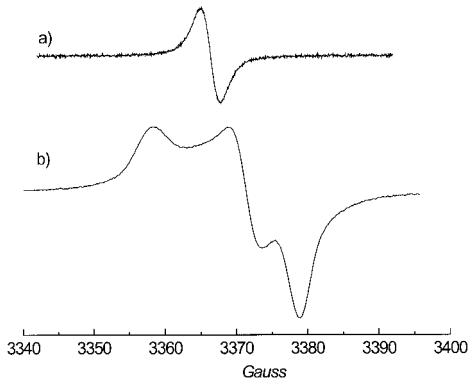

Figure 1. X-band EPR spectra of compound **14** in acetone solution at 293 K (a) and frozen CH_2Cl_2 solution at 110 K (b).

Spin counting experiments in 3×10^{-3} M solution in CH_2Cl_2 show that only $\approx$2% of the molecules exist in a radical form at room temperature. Taking into account this low concentration of the radical species we were careful to ensure that

the signal does not originate from impurities. One can speculate that in spite of mildly basic conditions in the synthesis of **14** and **16**, certain acidic impurities could cause the appearance of the signal of the TTF radical cation,[20] but this is incompatible with any basic impurity which would need to be present to form the radical anion of the fluorene nucleus. Model compounds, **6** and **11**, do not give any significant signal, although they were synthesized under the same conditions (and might, therefore, be expected to contain the same impurities, if any). Finally, the intensity of the signal from **14** did not change upon exposure to sunlight for 1 h, thus ruling out the possibility of a photoinduced electron transfer.

The intensity of the signal from the powdered samples of **14** increases as the temperature decreases (Figure 2) and no maxima were found down to 10 K. It is noteworthy that the

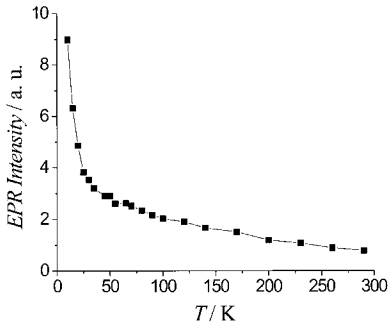

Figure 2. Temperature dependence of the intensity of EPR signal for a powdered sample of **14**.

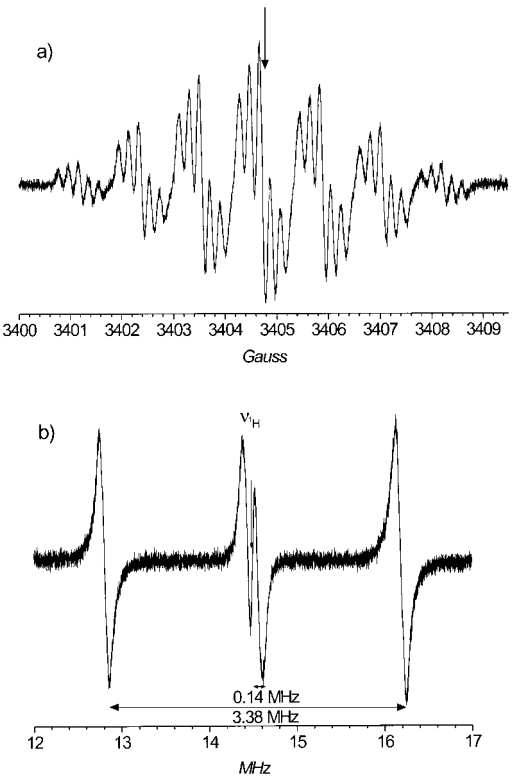

Figure 3. X-band EPR spectrum (a) and ENDOR spectrum (static field corresponding to the middle of the EPR multiplet) (b) of **24** in MeCN/toluene (3:2 *v*/*v*) solution at 285 K.

intermolecular complex **TTF**:**22**, which was shown by X-ray analysis to form alternating DADA stacks and to have only partial charge transfer,[7] gives rise to a very similar EPR signal with the same *g* values in the solid state.

From these data we conclude that the origin of the EPR signal of **14** is the ground (not thermoexcited) state. Most probably, the intense signal in the solid state results from an *inter*molecular self-complex [e.g. $(\mathbf{14})_2$], whereas in solution this kind of complex would readily dissociate, so only 2 % spin concentration is found.[24] Therefore, in the absence of the *inter*molecular complexation, the ground state of compound **14** is neutral.

The Li^+ salt of the fluorene radical anion, **24**, gives a well resolved EPR spectrum in MeCN/toluene solution at room temperature, centered at $g = 2.0030$, and the best resolution was achieved at 285 K (Figure 3a). In frozen solution, and as a powdered sample, **24** gives rise to an axial spectrum with $g_{1,2} = 2.0030$ and $g_3 = 2.0026$. Copper salt **25** gives a broad signal with $g = 2.003$; no evidence was found for the presence of a paramagnetic Cu^{II} ions in the sample. The solution ENDOR spectrum of **24** (Figure 3b) reveals two distinct ^1H couplings of 3.38 and 0.14 MHz (1.21 and 0.05 G, respectively); ^{14}N coupling was not observed in the ENDOR spectra. The EPR spectrum could be simulated well with hyperfine couplings of (number of equivalent nuclei in parentheses) a_H (2) = 3.38 MHz, a_H (2) = 0.14 MHz, a_N (2) = 3.25 MHz, a_N (2) = 0.51 MHz, and a Lorentzian linewidth of 0.1 G. A third set of two equivalent ^{14}N nuclei is present in **24**, however, these were not resolved due to a very weak coupling. We assign the larger of the ^1H couplings (3.25 MHz) to the 3-, 6-positions of the fluorene ring, in accord with the PMB observed for similar fluorene compounds (see above). The 0.14 MHz coupling belongs to the protons at the 1-, 8-ring positions. According to the McConnell equation,[25] the unpaired electron density in the C $2p_z$ orbitals contributing to the π-system was calculated from the a_H values to be ≈5 % of the unpaired electron density on each of the C3 and C6 positions and ≈0.2 % on each of C1 and C8. The crude estimation[26] of the unpaired π-electron density at the two sets of two ^{14}N nuclei gives ≈4 and 0.1 %, but we cannot unambiguously assign these.

The observed paramagnetism of **14** prompted us to measure the electrical conductivity. Earlier, metallic conductivity was found in a 2:1 CTC of fluorene **22** with bis(ethylenedioxy)-TTF ($\sigma_{rt} = 18\ S\,cm^{-1}$, in compressed pellets), but when a 1:1 complex was formed (with fluorene **1**), only weak semiconductivity was observed ($\sigma_{rt} \approx 10^{-10}\ S\,cm^{-1}$).[27] For the diads **14** and **16** with 1:1 stoichiometry no observable conductivity was found from their compressed pellets ($\sigma_{rt} < 10^{-8}\ S\,cm^{-1}$, two-probe method).

Consistent with the X-ray data (see below) which shows no long-range stacking, the copper salt **25** is an electrical insulator ($\sigma_{rt} < 10^{-8}\ S\,cm^{-1}$). In contrast to **25**, semiconductive behavior was shown by the lithium salt **24** ($\sigma_{rt} = 1 \times 10^{-3}\ S\,cm^{-1}$, $\sigma_{200\,K} = 3 \times 10^{-5}\ S\,cm^{-1}$). Such relatively high conductivity is unexpected for a 1:1 salt with complete charge transfer,[28] and is, probably, an effect of doping by traces of neutral fluorene **22**.

© 2002 WILEY-VCH Verlag GmbH & Co. KGaA, Weinheim
0947-6539/02/0820-4660 $ 20.00+.50/0 *Chem. Eur. J.* **2002**, *8*, No. 20

Electrochemistry: The cyclic voltammetry (CV) of the diads **13**–**16**, **18** and **19** in CH_2Cl_2 is characterized by clear multiredox amphoteric behavior (Figure 4) consisting of two

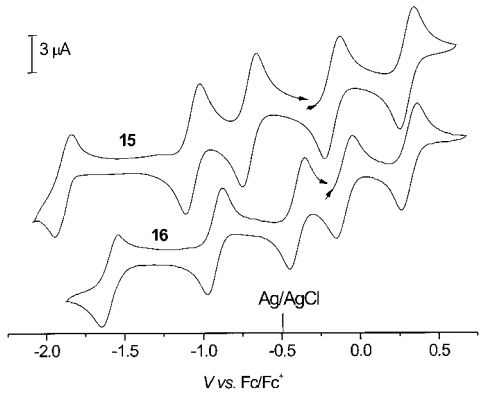

Figure 4. CV of compounds **15** and **16** measured in CH_2Cl_2 at 50 mV s^{-1}.

reversible single-electron oxidation waves yielding a radical cation and dication state of the TTF moiety, and three reversible single-electron reductions of the fluorene fragment, which afford a radical anion, dianion and radical trianion species:

$$D^{2+}-\sigma-A \rightleftharpoons D^{\bullet+}-\sigma-A \rightleftharpoons D-\sigma-A \rightleftharpoons D-\sigma-A^{\bullet-} \rightleftharpoons D-\sigma-A^{2-} \rightleftharpoons D-\sigma-A^{\bullet 3-}$$

The thermodynamic potentials E^0 are given in Table 1, together with data for compounds **3**, **6**–**8**, **10** and **12** to show the mutual influence of the TTF and fluorene fragments. As expected,[7] the conversion of the keto group into the dicyanomethylene group (**3b** → **6**, **13b** → **14**, **15** → **16**, **18** → **19**) results in a significant positive shift in the reduction potentials with larger shifts being observed for $E_{1red}{}^0$ (290–370 mV) and $E_{3red}{}^0$ (190–310 mV) than for $E_{2red}{}^0$ (70–160 mV). Also, the thermodynamic stability of the derived radical anions of the dicyanomethylene derivatives (which relates to the disproportionation equilibrium $2A^{\bullet-} \rightleftharpoons A + A^{2-}$) is consistently higher than that of the fluorenone precursors (Table 1). As for the TTF moiety, a very predictable decrease or increase in its donor ability was found upon the attachment of the electron withdrawing CHO (**7** → **8**) or electron releasing CH_2OH (**7** → **10**) groups. Less predictably, an increase in the $E_{1ox}{}^0$ values followed the acylation of alcohol **10** to yield **11**, possibly as a result of a "through-space" effect of the $CH_2OC(O)R$ substituent. This kind of behavior was noted earlier for $TTFCH_2OC(O)Ph$.[29]

For the "**b**" series possessing the longer σ-bridge, the attachment of the TTF moiety to the fluorenone (**3b** → **13b**, **3b** → **15**) has no apparent influence on the acceptor ability of the fluorene unit, whereas the same change for the dicyanomethylene analogues (**6** → **14**, **6** → **16**) results in a 60–70 mV negative shift of the first reduction potential; this indicates an interaction between the donor and acceptor moieties in compounds **14** and **16**. There is a concomitant 40–70 mV positive shift in the $E_{1ox}{}^0$ value of TTF due to the presence of the fluorenedicyanomethylene fragment (**11** → **14**, **15** → **16**). In the shorter-bridge series "**a**" the D/A interaction is also observable in fluorenone **13b** manifested in the 20/60 mV

Table 1. Data from CV measurements.[a]

Compound	$E_{1ox}{}^0$/V	$E_{2ox}{}^0$/V	$E_{1red}{}^0$/V	$E_{2red}{}^0$/V	$E_{3red}{}^0$/V	$\log K_{dispr}$[b]	ΔE/ eV[c]
3a	–	–	−0.64	−1.01	−1.50	−6.3	–
3b	–	–	−0.68	−1.05	−1.87	−6.3	–
6	–	–	−0.31	−0.91	−1.57[d]	−9.8	–
7	−0.15	0.32	–	–	–	–	–
8	0	0.52	–	–	–	–	–
9	−0.05	0.41	–	–	–	–	–
10	−0.23	0.24	–	–	–	–	–
11	−0.13	0.40	–	–	–	–	–
12	−0.22	0.30	–	–	–	–	–
13a	−0.07	0.40	−0.66	−1.01	−1.58[e]	−5.9	0.59
13b	−0.13	0.37	−0.68	−1.04	−1.86	−6.1	0.55
14	−0.09	0.35	−0.39	−0.90	−1.57	−8.6	0.30
15	−0.17	0.31	−0.69	−1.06	−1.84	−6.3	0.52
16	−0.10	0.32	−0.38	−0.90	−1.56	−8.8	0.28
18	−0.11	0.40	−0.72	−1.00	−1.81	−4.7	0.66
19	−0.10	0.41	−0.39	−0.93	−1.62	−9.2	0.29

[a] 0.2 M Bu_4NPF_6 in CH_2Cl_2, vs. Fc/Fc^+; [b] $\log K_{dispr} = -(E_{1red}{}^0 - E_{2red}{}^0)/0.059$; [c] ref. [30]; [d] this compound in MeCN showed four reversible reduction waves: $E_{1red}{}^0 = -0.24$ V, $E_{2red}{}^0 = -0.85$ V, $E_{3red}{}^0 = -1.48$ V, $E_{4red}{}^0 = -1.97$ V; [e] this wave was irreversible due to rapid degradation of the derived radical trianion.

shift of $E_{1ox}{}^0$ and $E_{1red}{}^0$ as compared to the model donor/acceptor compounds **3a** and **11** (see also the following Section). As the ICT π–π interaction is not possible in the shortest-bridge diads **18** and **19**, the donor ability of the TTF fragment in these compounds is not perturbed (within 10 mV) by the keto → dicyanomethylene transformation. In accordance with the fact that this charge-transfer interaction should disappear with reduction of the acceptor fragment to the radical anion, the presence of the TTF moiety has no influence on the second and third reduction waves of the fluorene nuclei.

It is remarkable that the difference between the oxidation and reduction potentials ($E_{1ox}{}^0 - E_{1red}{}^0$) for compounds **14**, **16** and **19** is as small as 280–300 mV, which represents the smallest solution HOMO–LUMO gap (≈0.3 eV[30]) so far reached for closed-shell organic compounds.

Electronic absorption spectra: Charge transfer interactions in the diads are also manifested in broad absorption bands in their visible and near-IR electronic spectra, with the maxima and intensities strongly dependant on the solvent used. These bands were not observed in solutions of either the separate donor (**11**) or acceptor (**4** or **6**) components, or their radical

Table 2. ICT bands in electronic absorption spectra of the diads.

Compound	Solvent	$\lambda_{CT\text{-}1}$/ nm (ε/M^{-1}cm^{-1})	$\lambda_{CT\text{-}2}$/ nm (ε/M^{-1}cm^{-1})
13a	CH_2Cl_2	1045 (550)	765 (700)
	acetone	920sh (440)	715 (550)
13b	CH_2Cl_2	990 (260)	750 (300)
	acetone	900sh (130)	705 (150)
15	CH_2Cl_2	975sh (240)	775 (260)
	acetone	920sh (150)	725 (170)
18	acetone	900sh	630sh
14	CS_2	1230 (4200)	800
	CH_2Cl_2	1230 (4700)	800 (2000)
	acetone		790 (850)
16	CH_2Cl_2	1260 (3400)	800 (1350)
19[33]	CH_2Cl_2	1200–1330	785–825

 © 2002 WILEY-VCH Verlag GmbH & Co. KGaA, Weinheim 0947-6539/02/0820-4661 $ 20.00+.50/0

ions (see the spectroelectrochemical experiments below), but a very similar spectrum was obtained for an intermolecular complex **TTF**:**22** (Figure 5). The increase in the acceptor character on conversion from the fluorenone (**13**, **15** and **18**) to the dicyanomethylene derivatives (**14**, **16** and **19**) results in a bathochromic shift and a substantial increase in the intensity of the CT bands indicating a much stronger donor–acceptor interaction in the latter series, in accordance with the CV results.

The concentration dependence of the intensity of the CT bands confirmed their intramolecular nature. A linear dependence ($r > 0.999$) was established for compounds **13**–**16** in acetone and CH_2Cl_2 over a wide range of concentrations

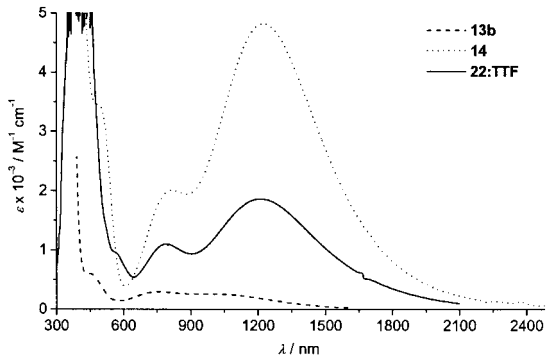

Figure 5. Electronic spectra of compounds **13b**, **14** (in CH_2Cl_2) and CTC **22:TTF** (in PhCN).

(10^{-3}–10^{-5} M), but little deviation was seen in the high concentration ($\geq 10^{-3}$ M) region, especially in a less polar solvent (CS_2).[31] This suggests that, even though the intramolecular charge transfer process dominates in these molecules, intermolecular complexation giving rise to a similar CT absorption can also take place at high concentrations. We suggest that these low energy bands arise from a π–π through-space charge transfer process involving an intramolecularly "head-to-tail" complexed state of the molecules. Geometry optimization using semiempirical PM3 methods for **14** shows that a folded "head-to-tail" conformation where the ICT interaction can take place is not only geometrically allowed but also is almost equal in energy to the linear conformation ($\Delta H = 23.0$ and 22.4 kcal mol^{-1}, respectively[32]). Interestingly, the ICT bands of fluorenone **13a** with the shorter σ-bridge are more than twice as intense as those of **13b**, which suggests a more efficient CT interaction in the former, in agreement with the CV results. The behavior of the shortest σ-bridge diads **18** and **19** (the geometry of which preclude intramolecular complexation) further corroborates the π–π "through-space" origin of the CT bands: the change in solution absorbance as a function of concentration (order > 1)[33] and almost no absorption at concentrations below 10^{-4} M indicates that only the intermolecular CT complex is responsible for the long-wavelength absorption in these diads.

It appears, therefore, that being separated by a σ-bridge the donor and acceptor moieties in these TTF–fluorene diads behave essentially as independent molecules giving rise to very similar manifestations of inter- and intramolecular interactions. In many cases these are concurrent processes which can be modulated by variations in the diad concentration and the flexibility of the σ-bridge.

The apparent discrepancy between the electrochemical HOMO–LUMO gap and $h\tilde{\nu}$(ICT) (ca. 1 eV) arises from the fact that ICT occurs solely in a CT complex, whereas CV data characterise uncomplexed or equilibrium states; the HOMO–LUMO orbital interactions in the former should increase the gap proportionally to the degree of interaction.

Spectroelectrochemistry: Compounds for which color and transparency in the visible/near-IR regions can be changed by applying various potentials (electrochromic materials) are of great current interest.[34] Some of them have found commercial applications, for example in information displays and self-darkening rear-view mirrors for cars.[35] For **14** and **16** the relatively high intensity of the ICT band at λ_{max} 1200 nm tailing to beyond 2000 nm, which was expected to vanish with oxidation/reduction of the D/A fragments, led us to study their electrochromism. Applying a potential stepwise up to +0.6 V (vs Pt wire quasireference electrode), to generate the radical cation, resulted in the complete disappearance of the near-IR ICT bands; instead, two bands characteristic of the TTF radical cation (λ_{max} 460 and 645 nm) arose (Figure 6a) and the solution changed its color from brown to green.[36] At more positive potentials (0.95 V) the long wavelength bands (460 and 645 nm) disappeared and the solution turned yellow indicating the formation of the dication species (λ_{max} 428 nm, Figure 6b). Analogously, switching to −0.6 V gave rise to the radical anion and the corresponding spectral change[37] (new bands at λ_{max} 315, 515 and 780 nm and a low intensity broad band at λ 900–1900 nm) made the solution violet (Figure 6c). The formation of the dianion species while scanning down to −1.5 V was monitored by loss of the characteristic vibronic band at 515 nm, an increase in the intensity of the near-IR band and the appearance of two new bands at λ_{max} 360 (shoulder) and 440 nm, although the radical trianion species can contribute to the spectrum at this potential (Figure 6d).

The two oxidation and the first two reduction processes were completely reversible for compound **16**, that is the initial spectra returned after re-setting the potential to +0.2 V and the system can be cycled between these five redox states for at least a few hours. The radical trianion state and also the dication and dianion states for **14** were partly irreversible (presumably, due to the lower stability of the linking ester compared with the amide bond): the prolonged exposure to redox potentials generating those states lead to partial decomposition of the compounds manifested in the reduced intensity of the ICT band on a reverse scan. The intensities of the bands belonging to the ionic states did not change, however, which indicates that the linking bonds (ester or amide) and not the donor/acceptor moieties were the sites of decomposition. We believe that compound **16** is a very promising electrochromic material by virtue of having five redox states ($2-$, $\cdot-$, 0, $\cdot+$, $2+$) each with distinctive visible/near-IR absorption spectra.

X-Ray analysis: TTF–fluorene-9-one derivative **18** was the only diad molecule to afford crystals suitable for X-ray analysis. The fluorenone moiety in **18** adopts a slightly twisted

 © 2002 WILEY-VCH Verlag GmbH & Co. KGaA, Weinheim 0947-6539/02/0820-4662 $ 20.00+.50/0 *Chem. Eur. J.* **2002**, *8*, No. 20

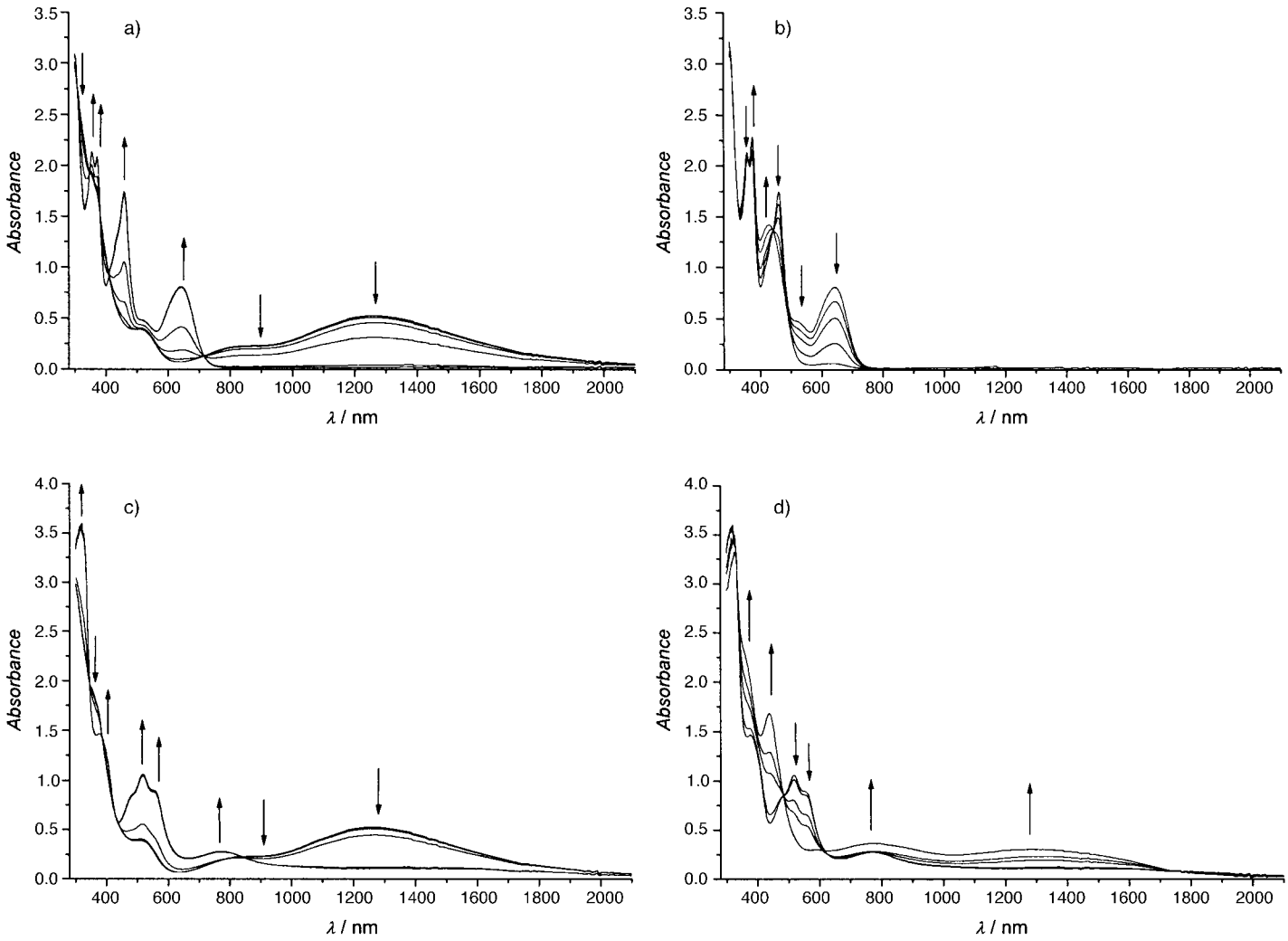

Figure 6. Spectroelectrochemical data for **16**: the formation of $\mathbf{16}^{\bullet+}$ (a), $\mathbf{16}^{2+}$ (b), $\mathbf{16}^{\bullet-}$ (c), $\mathbf{16}^{2-}$ (d).

conformation, due to the repulsion between the carboxy and nitro groups in positions 4 and 5, respectively, typical for 4,5-disubstituted fluorene derivatives (Figure 7). The TTF moiety is folded along the S(1)···S(2) and S(3)···S(4) vectors by 2.4° and 10.8° and twisted by 2.6° around the central C(15)=C(18) bond. As suggested from the electronic spectra in solution, there are no intramolecular contacts between donor and acceptor moieties: the TTF–fluorenone part of the molecule is roughly planar. These parts of two molecules contact face-to-face: in the resulting dimer the donor (TTF) unit of one molecule overlaps with the acceptor (fluorenone) unit of another giving rise to a CT band, responsible for the black color of the crystals. The dimers pack in a herringbone (edge-to-face) manner, without any continuous stacks. The packing leaves vast cavities, occupied by *n*-pentyl chains, which are disordered between different orientations, partially superimposed with similar chains of adjacent molecules and with acetone molecules of crystallization (in a non-stoichiometric occupancy). In the TTF moiety, all the C–S bonds are essentially equal (average 1.760(4) Å) and so are all the C=C bonds (average 1.347(5) Å); their lengths are characteristic for neutral TTF, indicating very little (or no) charge transfer in this diad.

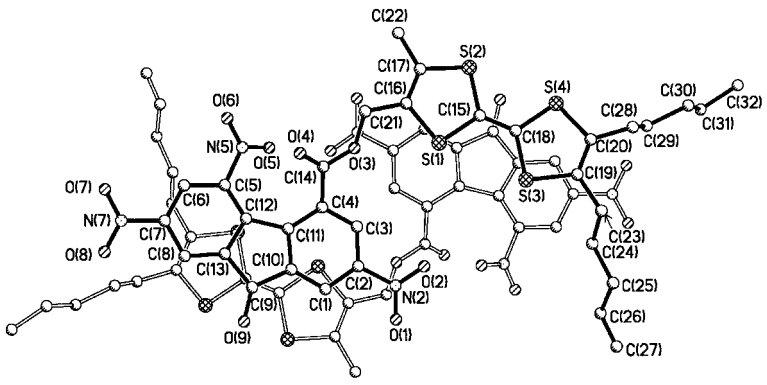

Figure 7. Dimer of compound **18** showing an overlap of TTF and fluorene moieties in the crystal (minor positions of the disordered *n*-pentyl chains are not shown).

The asymmetric unit of **25**·2MeCN contains two anion

 © 2002 WILEY-VCH Verlag GmbH & Co. KGaA, Weinheim 0947-6539/02/0820-4663 $ 20.00+.50/0

radicals of **22** (i and ii), each of them bridging two copper atoms through both cyano groups. Anion radicals of type i link Cu(1) and its equivalents, related through a 2_1 axis, into an infinite chain (Figure 8); anion radicals of type ii link Cu(2)

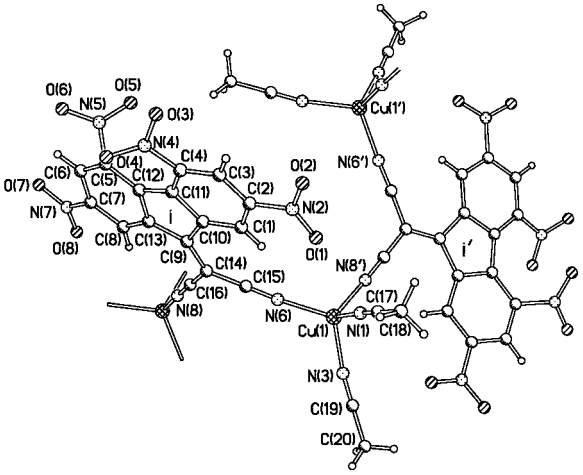

Figure 8. Chains in the structure of **25**·2MeCN. Primed atoms are generated by a 2_1 axis. Bond lengths [Å]: Cu(1)–N(1) 2.003(2), Cu(1)–N(3) 1.991(2), Cu(1)–N(6) and Cu(1)–N(8′) 1.990(2).

and its inversion equivalent into a closed dimer (Figure 9). The coordination of each copper atom in **25** is completed by two linear acetonitrile ligands forming a distorted tetrahedron (Cu-N-Me angles 170.2(2) to 176.8(2)°). The shortest Cu ··· Cu distances are 7.369(1) Å in the chain and 6.967(1) Å in the dimer.

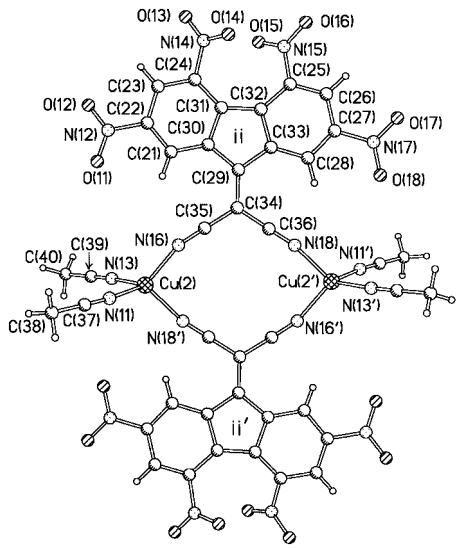

Figure 9. Dimers in the structure of **25**·2MeCN. Primed atoms are generated by an inversion centre. Bond lengths [Å]: Cu(2)–N(11) 2.002(2), Cu(2)–N(13) 1.993(2), Cu(2)–N(16) 1.987(2), Cu(2)–N(18′) 1.994(2).

The bond lengths in both anion radicals are essentially equal; a comparison with the neutral molecule in pure **22**[38] and in its PhCl solvate[39] (Table 3) shows a) increased π-conjugation in the five-membered ring; b) weakening of the C(9)=C(14) bond and c) strengthening of the adjacent C–CN bonds in **25**, similar to that observed in the TCNQ anion radical.[40] The fluorene nucleus in $\mathbf{22}^{\bullet-}$ is more planar than in neutral **22** (the deviation of thirteen fluorene carbon atoms from their mean plane averages 0.078 Å in moiety i and 0.055 Å in ii, versus 0.115 Å in **22**·PhCl), but the twist around the C(9)=C(14) bond (3.2° in i, 8.0° in ii) is slightly higher than in **22** or **22**·PhCl (ca. 2°). The anion radical i is disordered: two conformers with opposite tilts of the nitro groups occupy the same site with a ca. 9:1 ratio (Figure S11). The coordination of the cyano groups is nearly linear, the Cu-N-C angles are wider in the chain than in the dimer [average 172.9(2) and 165.3(2)°]. In both cases, the anion radical and the two coordinated copper atoms are approximately coplanar. Thus, in the dimer the $Cu_2(\mathbf{22})_2$ system is planar, but in the chain each two adjacent anion radicals are nearly perpendicular to each other. It is instructive to compare **25**·2MeCN with two recently studied polymorphs of [TCNQ]Cu salt,[41] where the distorted tetrahedral coordination of copper(I) comprises four cyano groups of TCNQ with no additional ligands, while each TCNQ bridges four Cu atoms, giving rise to a three-dimensional framework. In the tetragonal polymorph (a good semiconductor, $\sigma_{rt} = 0.25\ S\,cm^{-1}$, band gap 0.137 eV) TCNQ anion radicals of both frameworks form infinite stacks with interplanar separation of 3.24 Å. In the monoclinic form (poor semiconductor, $1.3 \times 10^{-5}\ S\,cm^{-1}$, band gap 0.332 eV) these moieties pack in a brickwork mode—parallel but poorly overlapping. The structure of **25**·2MeCN contains face-to-face pairs of anion-radicals **22** (one of type i and another of type ii, see above) contacting each other in an edge-to-face (herringbone) fashion, but no continuous stacks exist, which explains the absence of conductivity.

Table 3. Average bond lengths [Å].

Bonds[a]	**22**[b]	**22**·PhCl[c]	**23a**	**25**·2MeCN
C(9)–C(14)	1.354(15)	1.357(2)	1.405(5)	1.413(2)
C(9)–C(10)	1.470(9)	1.480(2)	1.447(5)	1.450(3)
C(10)–C(11)	1.411(12)	1.419(2)	1.435(5)	1.445(3)
C(11)–C(12)	1.478(6)	1.483(2)	1.454(4)	1.449(3)
C(14)–CN	1.436(9)	1.444(2)	1.457(5)	1.423(3)
C(14)–C(16)	–	–	1.411(5)	–
C(16)–CN	–	–	1.426(5)	–
C≡N	1.140(10)	1.147(2)	1.145(5)	1.153(3)

[a] Averaged with all chemically equivalent bonds; [b] at room temperature;[38]; [c] at 150 K.[39]

The asymmetric unit of K[**23**]·H_2O·½Me_2CO (**23a**) comprises two potassium cations, one terminal and one μ_2-aqua ligand, one μ_2-acetone ligand and two anions **23**, both μ_2-bridging in the same manner, via two cyano groups (Figure 10). The primary structural unit is a dimer, in which K(1) and K(2) atoms are bridged by two anion radicals, one aqua ligand [O(9)] and the acetone oxygen O(19), with K(1) coordinating also one terminal aqua ligand [O(10)]. The environment of K(2) is completed to form a distorted octahedron by two nitro oxygen atoms, O(7) and O(11), belonging to different dimers but strongly coordinated. The coordination of K(1) can be described as a tetragonal pyramid with O(9) in the apical position, completed to a distorted

© 2002 WILEY-VCH Verlag GmbH & Co. KGaA, Weinheim
0947-6539/02/0820-4664 $ 20.00+.50/0 *Chem. Eur. J.* **2002**, *8*, No. 20

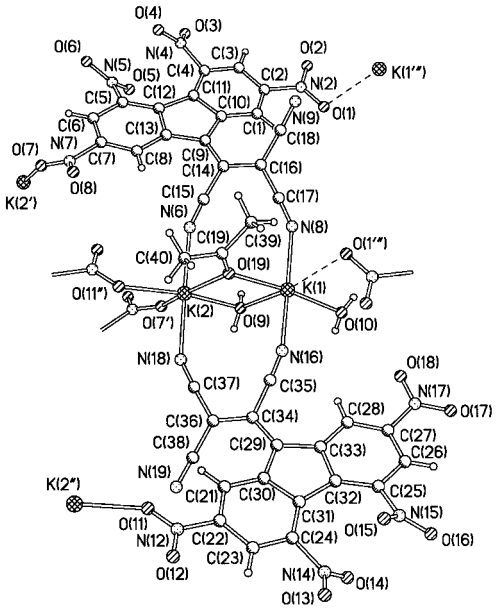

Figure 10. Crystal structure of K[**23**]·H_2O·½Me_2CO (**23a**). Bond lengths [Å]: K(1)–N(8) 2.398(4), K(1)–N(16) 2.409(4), K(1)–O(9) 2.446(3), K(1)–O(10) 2.262(3), K(1)–O(19) 2.405(3), K(1)–O(1‴) 2.728(3), K(2)–N(6) 2.497(4), K(2)–-N(18) 2.481(4), K(2)–O(9) 2.391(3), K(2)–O(19) 2.335(3), K(2)–O(7′) 2.429(3), K(2)–O(11″) 2.423(3). The disorder of the nitro groups at C(24) and C(25) is not shown.

octahedron by a much weaker interaction with a nitro oxygen atom O(1) of another dimer.

One of the fluorene anions displays the same disorder of the nitro groups as observed in **25**·2MeCN, also in a 9:1 ratio. Puckering of the fluorene moieties in **23a** is similar in magnitude and kind to that in **25**·2MeCN, the deviation of the carbon atoms from the mean plane averaging 0.07 Å. However, steric demands of the additional cyano group cause a substantial twist around the C(9)=C(14) bond (24 and 25°) and the C(14)–C(16) bond (20 and 15°). In spite of the twist, there is π-delocalization through the C(9)-C(14)-C(16)$(CN)_2$ moiety, which does not involve the C(15)N(6) cyano group. Similar delocalization was observed in donor-tricyanoethylene systems, for example N-substituted 1-amino-1,2,2-tricyanoethylene,[42] or 1-(*N*-pyridino)benzoylmethylene-1,2,2-tricyanoethylene.[43] In **23a**, as in **25**·2MeCN, the five-membered fluorene ring acquires almost aromatic character. Thus, in both complexes, negative charge is extensively delocalized between the fluorene nucleus and the cyano-containing substituent in the 9-position.

Conclusion

We have synthesized TTF–σ–fluorene compounds possessing both strong π-electron donor and acceptor moieties which provide rare examples of non-photoinduced electron transfer in donor–acceptor diads.[3d] Their redox behavior is fully reversible and comprises two single-electron oxidation and three single-electron reduction waves. Compounds **14**, **16** and **19** possess a HOMO–LUMO gap (≈0.3 eV in solution) which is the lowest reported for closed-shell monomeric organic compounds. Significant charge-transfer (ca. 0.6 electrons in the solid state) in compound **14**, **16** and **19** is manifested in a lowering of the C≡N stretching in the IR spectra, a strong EPR signal (in the solid state) and intense ICT bands in the near-IR region of their electronic spectra (in solution). Although the ground state of these diads in dilute solution is essentially neutral, *inter*molecular self-complexation in the solid state (and in concentrated solutions) gives rise to a strong ground-state EPR signal. Compounds **14** and **16** show distinctive electrochromism; the remarkable stability of five differently colored redox states of **16** (0, ·+, 2+, ·−, and 2−) makes it a promising electrochromic material for the near-IR spectral region. As shown by X-ray (for **18**) and spectroscopic analyses, in the shortest-bridge diads (**18** and **19**) no "through space" intramolecular donor–acceptor interaction is possible, which is an advantage for molecular rectification applications.[4]

Experimental Section

General methods: EPR spectra were recorded on Bruker ESP 300E Q-band or EMX X-band spectrometers. Solid state variable temperature (300–10 K) studies on **14** were performed at Q-band under non-saturating conditions determined at 10 K (0.1 mW microwave power; 100 kHz and 5 G modulation frequency and amplitude, respectively). Spin counting experiments on **14** in CH_2Cl_2 were performed at X-band and room temperature by calibration against a range of concentrations of standard dpph solutions in benzene measured under identical, non-saturating conditions. The experimental protocol was tested for accuracy against solutions of known concentration of other radical species. ENDOR spectra were measured using a Bruker ER 200 ENB ENDOR cavity with a field modulation frequency of 12.5 kHz. The spectrometer was fitted with a Bruker VT 2000 variable temperature system; an ER033 M field frequency lock, which was used for multiple EPR acquisitions and ENDOR experiments. Accurate field measurements were made using a single sweep with a Bruker 035 NMR Gaussmeter (corrected using a sample of the perylene radical cation in conc. H_2SO_4, $g = 2.002569 \pm 0.000006$). ENDOR spectra were obtained with the above system fitted with a Bruker ESP 360 DICE ENDOR system using RF modulation (again with frequency 12.5 kHz) and an ENI A-300 RF power amplifier operating at an attenuation of 8 dB (ca. 200–400 W). Concentrations of ≈ 10^{-3} M were used for all solution EPR and ENDOR measurements.

Cyclic voltammetry experiments were performed at ambient temperature with a BAS CV50 electrochemical analyzer, in a three-electrode cell (Ag/$AgNO_3$ in MeCN reference) using 1.6 mm diameter platinum disk as a working electrode. 0.2 M Bu_4NPF_6 in CH_2Cl_2 was used as the electrolyte. All the potentials (except in the spectroelectrochemical section) are quoted vs. the ferrocene/ferrocenium (Fc/Fc^+) couple, which was used as the internal standard except when it overlapped with the oxidation peaks of the sample. The Fc/Fc^+ couple showed 0.21 V (vs $Ag/AgNO_3$) and 0.50 V (vs Ag/AgCl).

Spectroelectrochemical data were recorded for compounds **3b**, **6**, **11**, **14** and **16** (ca. 10^{-4} M) in MeCN and CH_2Cl_2 with Bu_4NPF_6 (0.1 M) as supporting electrolyte on a Varian Cary 5 spectrophotometer between 250–2300 nm at ambient temperature. Spectra were corrected for background absorption arising from the cell, the electrolyte and the working electrode. The OTTLE cell used a Pt gauze working electrode, Pt wire counter and pseudo reference electrodes. The solutions were analyzed in situ: the working electrode was held at a potential at which no electrochemical work was being done in the cell and the spectrum of the neutral compound was recorded, which was identical to the spectrum recorded for open-circuit conditions. The potential was then increased in 50–200 mV increments and held until equilibrium had been obtained, as evidenced by a sharp drop in the cell current. The cell was based upon that described elsewhere,[44] and was driven by a home-built potentiostat.

Table 4. Crystal data and experimental details.

Compound	**18**[a]	**23a**	**25**·2MeCN
formula	$C_{32}H_{31}N_3O_9S_4\cdot\frac{1}{4}C_3H_6O$	$C_{39}H_{18}K_2N_{14}O_{19}$	$C_{40}H_{20}CuN_{16}O_{16}$
F_w	744.36	1064.87	1107.80
T [K]	120	120	110
symmetry	monoclinic	triclinic	monoclinic
space group	$I2/a$ (no. 15)	$P\bar{1}$ (no. 2)	$P2_1/c$ (no. 14)
a [Å]	15.719(5)	8.714(3)	14.2240(7)
b [Å]	12.586(4)	15.364(4)	10.2424(6)
c [Å]	37.231(13)	17.161(5)	29.7103(15)
α [°]	90	78.57(1)	90
β [°]	95.49(1)	76.74(1)	96.270(3)
γ [°]	90	74.80(1)	90
V [Å^3]	7332(4)	2134.6(11)	4302.5(4)
Z	8	2	4
refls collected	43576	26957	39493
unique refls	9722	11157	8895
R_{int}.	0.050	0.035	0.048
refls $F^2 > 2\sigma(F^2)$	6646	8075	7167
$R[F^2 > 2\sigma(F^2)]$	0.070	0.084	0.038
$wR(F^2)$, all data	0.238	0.299	0.094

[a] Complex disorder of both *n*-pentyl chains. Atoms C(24) to C(27): occupancies 75% in positions A, 25% in B. Position A is superimposed with an acetone molecule (occupancy 25%), in which C and O atoms are statistically mixed in positions O/C(1S) and O/C(3S). Atoms C(29) to C(32) in positions A have occupancies of 50%, C(29B) and C(30B) have occupancies of 50%; C(31) and C(32) in positions B and C have occupancies of 25%. C(26B) lies on axis 2.

X-ray crystallography: X-ray diffraction experiments (covering full sphere of reciprocal space) were carried out on a SMART 3-circle diffractometer with a 1 K CCD area detector, using graphite-monochromated $Mo_{K\alpha}$ radiation ($\lambda = 0.71073$ Å) and a Cryostream (Oxford Cryosystems) open-flow N_2 gas cryostat. The structures were solved by direct methods and refined by full-matrix least squares against F^2 of all data, using SHELXTL software.[45] Crystal data and experimental details are summarized in Table 2, full structural information has been deposited with the Cambridge Crystallographic Data Centre as supplementary publications nos. CCDC-172395 (**18**), CCDC-168417 (**23a**) and CCDC-168416 (**25**·2MeCN).

Compounds **2b**–**5b** and **6** were prepared as described.[46]

2-(Methoxycarbonylmethylsulfanyl)-4,5,7-trinitrofluorene-9-one (2a): Methyl 2-mercaptoacetate (0.50 mL, 5.6 mmol) followed by $NaHCO_3$ (0.50 g, 5.9 mmol) were added to a solution of fluorenone **1** (0.71 g, 2.0 mmol) in MeCN (20 mL). The red-brown reaction mixture was stirred at 20 °C for 2 h and the solvent was removed in vacuo. The residue was purified by chromatography on silica gel eluting with CH_2Cl_2 to give pure sulfide **2a** (0.45 g, 54%[47]). M.p. 182–183 °C; ^{1}H NMR (300 MHz, $CDCl_3$): $\delta = 8.93$ (d, $J = 2$ Hz, 1H), 8.76 (d, $J = 2$ Hz, 1H), 8.05 (d, $J = 2$ Hz, 1H), 8.00 (d, $J = 2$ Hz, 1H), 3.89 (s, 2H), 3.82 (s, 3H); ^{13}C NMR (75 MHz, [D$_6$]acetone): $\delta = 185.5$, 168.3, 148.7, 146.8, 145.8, 145.7, 139.3, 137.62, 137.60, 129.1, 127.4, 125.9, 125.5, 122.4, 53.3, 34.3; MS (EI): *m*/*z* (%): 419 (100) $[M]^+$; elemental analysis calcd (%) for $C_{16}H_9N_3O_9S$: C 45.83, H 2.16, N 10.02; found: C 45.39, H 2.10, N 9.73.

2-(Methoxycarbonylmethylsulfonyl)-4,5,7-trinitrofluorene-9-one (3a): 33% Aqueous H_2O_2 (1 mL, excess) was added to a solution of sulfide **2a** (0.42 g, 1.0 mmol) in hot AcOH (20 mL) and the reaction mixture was stirred at 70 °C for 3 h. Two thirds of the solvent was evaporated in vacuo, then water (1.5 mL) was added and the solution was cooled to 5 °C. The precipitate was filtered off, washed with 80% AcOH, hot water and methanol giving a pale-yellow powder of **3a** (0.40 g, 89%). M.p. 176–177 °C; ^{1}H NMR (300 MHz, [D$_6$]acetone): $\delta = 9.06$ (d, $J = 2$ Hz, 1H), 8.87 (d, $J = 2$ Hz, 1H), 8.79 (d, $J = 2$ Hz, 1H), 8.66 (d, $J = 2$ Hz, 1H), 4.85 (s, 2H), 3.72 (s, 3H); ^{13}C NMR (75 MHz, [D$_6$]acetone): $\delta = 185.5$, 163.7, 151.2, 147.3, 147.2, 145.0, 139.9, 139.6, 138.4, 138.0, 131.9, 128.9, 126.7, 123.4, 59.9, 53. 4; MS (EI): *m*/*z* (%): 451 (4) $[M]^+$, 421 (22) $[M - NO]^+$, 405 (18) $[M - NO_2]^+$, 329 (100); elemental analysis calcd (%) for $C_{16}H_9N_3O_{11}S$: C 42.58, H 2.01, N 9.31; found: C 42.40, H 1.96, N 9.32.

2-(Hydroxycarbonylmethylsulfonyl)-4,5,7-trinitrofluorene-9-one (4a): Ester **3a** (74 mg, 0.164 mmol) was dissolved in TFA (5 mL) at reflux, water (8 mL) was added and the reaction mixture was refluxed for 6 h. Then it was evaporated in vacuo, the residue was triturated with chloroform (3 mL) and the precipitate was filtered off and dried in vacuo to give acid **4a** (48 mg, 68%) as a solvate **4a**·½CF_3CO_2H. M.p. >150 °C (decomp); ^{1}H NMR (300 MHz, [D$_6$]acetone): $\delta = 9.05$ (d, $J = 2$ Hz, 1H), 8.86 (d, $J = 2$ Hz, 1H), 8.80 (d, $J = 2$ Hz, 1H), 8.67 (d, $J = 2$ Hz, 1H), 4.81 (s, 2H); MS (CI): *m*/*z* (%): 411 (30) $[M+NH_4 - CO_2]^+$, 397 (10) $[M+NH_4 - CH_2CO_2]^+$, 381 (100); elemental analysis calcd (%) for $C_{15}H_4N_3O_{11}S\cdot\frac{1}{2}CF_3CO_2H$: C 37.66, H 1.48, N 8.23; found: C 37.31, H 1.57, N 8.46.

5-Methyl-4′,5′-dipentyltetrathiafulvalene-4-carbaldehyde (8): LDA (3 mL of a 1.6 M solution in THF/heptane, 4.8 mmol) was added at −78 °C to a solution of TTF derivative **7**[9] (1.44 g, 4.0 mmol) in anhydrous diethyl ether (50 mL), the reaction solution was stirred for 2 h at −78 °C followed by addition of *N*-methylformanilide (0.55 mL, 4.5 mmol). The reaction mixture was allowed to reach 20 °C overnight, then quenched with ice-water and neutralized with AcOH (ca. 0.9 mL). The organic layer was separated, washed with water and brine, dried over $MgSO_4$ and, after evaporation, was purified by chromatography on silica gel, eluting with ethyl acetate/petroleum ether (1:3 *v*/*v*). The red-violet fraction was evaporated and dried in vacuo to give aldehyde **8** (1.03 g, 66%) as a dark red solid. M.p. 54–57 °C; ^{1}H NMR (300 MHz, [D$_6$]acetone): $\delta = 9.77$ (s, 1H), 2.54 (s, 3H), 2.44 (t, $J = 7.5$ Hz, 4H), 1.58–1.45 (m, 4H), 1.40–1.26 (m, 8H), 0.89 (t, $J = 6$ Hz, 6H); ^{13}C NMR (75 MHz; [D$_6$]acetone): $\delta = 180.4$, 153.9, 134.3, 130.1, 129.7, 113.1, 103.7, 31.9, 30.20, 30.18, 29.2 (2C), 23.1 (2C), 14.27 (2C), 14.19; IR (nujol): $\tilde{\nu} = 1664$ (C=O), 1461, 1376, 722 cm^{-1}; UV/Vis (CH_2Cl_2): λ_{max} (ε) = 296 (12200), 495 nm (2000 M^{-1}cm^{-1}); MS (EI): *m*/*z* (%): 386 (100) $[M]^+$; elemental analysis calcd (%) for $C_{18}H_{26}OS_4$: C 55.92, H 6.78; found: C 55.78, H 6.79.

The by-product **9** (105 mg, 5%) was isolated from the last chromatography fraction as a dark red tar. ^{1}H NMR (500 MHz; [D$_6$]acetone): $\delta = 9.94$ (s, 1H), 7.42 (t, $J = 8$ Hz, 2H), 7.33 (d, $J = 13$ Hz, 1H), 7.29 (dd, $J = 1$, 8 Hz, 2H), 7.16 (t, $J = 8$ Hz, 1H), 6.54 (d, $J = 13$ Hz, 1H), 3.42 (s, 3H), 2.42 (t, $J = 7.5$ Hz, 4H), 1.58–1.45 (m, 4H), 1.40–1.26 (m, 8H), 0.89 (t, $J = 6$ Hz, 6H); ^{13}C NMR (75 MHz; [D$_6$]acetone): $\delta = 179.1$, 155.1, 147.3, 144.2, 130.4, 129.9, 129.5, 126.9, 125.0, 120.5, 114.0, 103.0, 94.1, 37.0, 31.9 (2C), 30.18, 30.16, 29.2 (2C), 23.0 (2C), 14.3 (2C); IR (KBr): $\tilde{\nu} = 1649$ (C=O), 1611, 1591, 1461, 1377, 1130, 722 cm^{-1}; λ_{max} (ε) = 259 (5900), 307 (7000), 336 (6000), 405 nm (10500), 495 (1800 M^{-1}cm^{-1}); MS (EI): *m*/*z* (%): 503 (100) $[M]^+$; elemental analysis calcd (%) for $C_{26}H_{33}NOS_4$: C 61.98, H 6.60, N 2.78; found: C 61.75, H 6.65, N 2.76.

4-Hydroxymethyl-5-methyl-4′,5′-dipentyltetrathiafulvalene (10): Sodium borohydride (70 mg, 1.84 mmol) was added to a solution of aldehyde **8** (0.56 g, 1.44 mmol) in dry EtOH and the reaction mixture was stirred at 20 °C for 1 h (the red color of **8** vanished within 10 min). Then ethyl acetate (20 mL) was added, the organic layer was washed with water and brine, dried over $MgSO_4$, and filtered through a 1 cm pad of silica gel. Evaporation of the filtrate gave alcohol **10** (0.52 g, 92%) as an amorphous solid. M.p. 59–62 °C; ^{1}H NMR (200 MHz; [D$_6$]acetone): $\delta = 4.42–4.30$ (m, 3H), 2.41 (t, $J = 7.5$ Hz, 4H), 1.99 (s, 3H), 1.60–1.42 (m, 4H), 1.42–1.24 (m, 8H), 0.90 (t, $J = 6$ Hz, 6H); ^{13}C NMR (50 MHz; [D$_6$]acetone): $\delta = 131.2$, 129.75, 129.68, 125.7, 108.1, 107.7, 58.1, 31.9, 30.2 (2C), 29.2 (2C), 23.1 (2C), 14.3 (2C), 13.6; MS (EI): *m*/*z* (%): 388 (100) $[M]^+$; elemental analysis calcd (%) for $C_{18}H_{28}OS_4$: C 55.92, H 7.26; found: C 55.79, H 7.25.

4-Acetoxymethyl-5-methyl-4′,5′-dipentyltetrathiafulvalene (11): Pyridine (0.08 mL, 0.10 mmol), followed by acetyl chloride (0.05 mL, 0.088 mmol) was added to a solution of alcohol **10** (65 mg, 0.0167 mmol) in dry MeCN (10 mL) and the reaction mixture was stirred at 20 °C for 2 h. After evaporation of the solvent in vacuo the residue was purified by chromatography on silica gel eluting with ethyl acetate/petroleum ether (2:5 *v*/*v*) affording **11** (64 mg, 89%) as an orange oil. ^{1}H NMR (200 MHz; [D$_6$]acetone): $\delta = 4.82$ (s, 2H), 2.42 (t, $J = 7$ Hz, 4H), 2.09 (s, 3H), 2.04 (s, 3H), 1.60–1.42 (m, 4H), 1.42–1.25 (m, 8H), 0.90 (t, $J = 6$ Hz, 6H); IR (nujol): $\tilde{\nu} = 1750$ (C=O), 1462, 1377, 1219, 722 cm^{-1}; MS (EI): *m*/*z* (%): 430 (100) $[M]^+$; elemental analysis calcd (%) for $C_{20}H_{30}O_2S_4$: C 55.77, H 7.02; found: C 55.47, H 6.78.

4-(*N*-Benzylaminomethyl)-5-methyl-4′,5′-dipentyltetrathiafulvalene (12): Aldehyde **8** (83 mg, 0.214 mmol), benzylamine (27 μL, 0.248 mmol) and molecular sieves 4 Å (300 mg) were refluxed in dry cyclohexane (5 mL) for 15 h, until TLC showed a complete conversion of the aldehyde. The reaction mixture was filtered and evaporated in vacuo. The residue was

© 2002 WILEY-VCH Verlag GmbH & Co. KGaA, Weinheim
0947-6539/02/0820-4666 $ 20.00+.50/0 *Chem. Eur. J.* **2002**, *8*, No. 20

dissolved in dry diethyl ether (5 mL) and $LiAlH_4$ (12 mg, 0.31 mmol) was added. The reaction mixture was stirred at 20 °C for 3.5 h (full conversion within 3 h was confirmed by TLC) and wet ethyl acetate was added slowly to quench the excess of $LiAlH_4$. After evaporation, the mixture was purified by chromatography on silica gel, eluting with petroleum ether/ethyl acetate mixture (5:1 *v*/*v*) to give amine **12** (88 mg, 88 %) as a pink solid. M.p. 67–68 °C; ^{1}H NMR (300 MHz, [D$_6$]acetone): $\delta = 7.40-7.27$ (m, 4H), 7.22 (tt, $J = 7$, 2 Hz, 1H), 3.77 (s, 2H), 3.52 (d, $J = 0.6$ Hz, 2H), 2.41 (t, $J = 7.5$ Hz, 4H), 2.2 (br s, N*H*$_2$), 1.91 (s, 3H), 1.58–1.45 (m, 4H), 1.40–1.27 (m, 8H), 0.90 (t, $J = 6.5$ Hz, 6H); ^{13}C NMR (75 MHz; [D$_6$]acetone): $\delta =$ 141.2, 130.9, 129.7, 129.6, 129.0, 128.9, 127.6, 124.7, 108.5, 107.4, 53.0, 46.5, 31.9, 30.1 (2C), 29.15, 29.14, 23.0 (2C), 14.2 (2C), 13.7; IR (nujol): $\tilde{\nu} = 1461$, 1376, 722 cm^{-1}; MS (EI): *m*/*z* (%): 477 (100) $[M]^+$, 372 (100) $[M-$PhCH$_2$N$]^+$; elemental analysis calcd (%) for $C_{25}H_{35}NS_4$: C 62.85, H 7.38, N 2.93; found: C 62.44, H 7.36, N 2.69.

Compound 13a: Acid **4a** (0.13 g, 0.30 mmol) was stirred in oxalyl chloride (1 mL) with DMF (1 μL) as a catalyst for 20 h. Then the volatile materials were removed in vacuo and the residual acid chloride **5a** was used immediately in the next step. A solution of alcohol **10** (117 mg, 0.30 mmol) and pyridine (70 μL, 0.87 mmol) in dry MeCN (15 mL) was added to acid chloride **5a** and the reaction mixture was stirred at 20 °C for 6 h. After removing the solvent in vacuo, the residue was triturated with methanol (3 mL), filtered and purified by chromatography on silica gel eluting with ethyl acetate/petroleum ether (1:3 *v*/*v*) to give product **13a** (72 mg, 30 %). M.p. 160 °C (decomp); ^{1}H NMR (300 MHz, [D$_6$]acetone): $\delta = 8.99$ (d, $J =$ 2 Hz, 1H), 8.86 (d, $J = 2$ Hz, 1H), 8.77 (d, $J = 2$ Hz, 1H), 8.54 (d, $J = 2$ Hz, 1H), 4.95 (s, 2H), 4.81 (s, 2H), 2.45–2.24 (m, 4H), 2.03 (s, 3H), 1.57–1.39 (m, 4H), 1.39–1.25 (m, 8H), 0.97–0.84 (m, 6H); IR (nujol): $\tilde{\nu} = 1731$ (C=O), 1615, 1541, 1343, 1192, 1119, 780 cm^{-1}; MS (ES+): *m*/*z* (%): 808 (30) $[M+H]^+$, 807 (25) $[M]^+$, 564 (100); elemental analysis calcd (%) for $C_{33}H_{33}N_3O_{11}S_5$: C 49.06, H 4.12, N 5.20; found: C 48.91, H 4.09, N 5.17.

Compound 13b: A solution of alcohol **10** (0.18 g, 0.46 mmol) and pyridine (0.10 mL, 1.2 mmol) in dry MeCN (15 mL) was added to acid chloride **5b** (0.225 g, 0.48 mmol), the reaction mixture was stirred at 20 °C for 6 h and the resulting gray-green precipitate was filtered off and thoroughly washed with acetonitrile, $NaHCO_3$/water, then water and, finally, methanol to give fluorenone **13b** (0.235 g, 62 %). M.p. 145 °C (decomp). The mother liquor was evaporated, the residue washed with methanol, hot hexane and purified by chromatography on silica gel, eluting with diethyl ether to give an additional portion of **12b** (0.03 g, 8 %). M.p. 145 °C (decomp); ^{1}H NMR ([D$_6$]acetone): $\delta = 9.04$ (d, $J = 2$ Hz, 1H), 8.82 (d, $J = 2$ Hz, 1H), 8.79 (br s, 1H), 8.63 (br s, 1H), 4.79 (s, 2H), 3.92 (t, $J = 7$ Hz, 2H), 2.96 (t, $J = 7$ Hz, 2H), 2.41 (m, 4H), 2.03 (s, 3H), 1.57–1.45 (m, 4H), 1.39–1.28 (m, 8H), 0.94–0.86 (m, 6H); IR (KBr): $\tilde{\nu} = 1735$ (C=O), 1617, 1542, 1343, 1192, 1139 cm^{-1}; MS (ES+): *m*/*z* (%): 821 (100) $[M]^+$; elemental analysis calcd (%) for $C_{34}H_{35}N_3O_{11}S_5$: C 49.70, H 4.26, N 5.12; found: C 49.67, H 4.28, N 4.90.

Compound 13b (alternative synthesis): Dicyclohexylcarbodiimide (17 mg, 0.083 mmol) was added to a suspension of acid **4b** (27 mg, 0.060 mmol) in dry CH_2Cl_2 (2.5 mL), the reaction mixture was stirred at 0 °C for 40 min. Alcohol **10** (27 mg, 0.069 mmol) followed by 4-dimethylaminopyridine (1 mg, 0.01 mmol) were added to this mixture which was stirred at 20 °C for 15 h. After filtering, the filtrate was purified by chromatography on silica gel, eluting with CH_2Cl_2/ethyl acetate (20:1 *v*/*v*). The green fraction was evaporated, the residue was triturated with MeCN (2 mL), filtered off, subsequently washed with MeCN, methanol and hexane to give **13b** (17 mg, 34 %) with spectral characteristics identical to those of the above sample.

Compound 14: Fluorenone **13b** (59 mg, 0.068 mmol) and malononitrile (59 mg, 0.89 mmol) were stirred in DMF (1 mL) for 6 h at 20 °C; the solution volume was reduced in vacuo to ≈0.3 mL, diluted with methanol (3 mL) and the precipitate was filtered off and washed with methanol yielding a brown powder (54 mg) which was purified by flash chromatography on silica gel eluting with ethyl acetate/petroleum ether (1:1 *v*/*v*) to give **14** (47 mg, 80 %). M.p. 150 °C (decomp); ^{1}H NMR (300 MHz; [D$_6$]acetone): $\delta = 9.5-9.0$ (br m, 4H), 4.73 (br m, 2H), 4.02 (br m, 2H), 3.07 (t, $J = 6$ Hz, 2H), 2.53 (br m, 4H), 2.1–1.8 (br m, 3H), 1.57–1.34 (m, 4H), 1.34–1.15 (m, 8H), 0.88–0.70 (m, 6H); ^{1}H NMR (300 MHz; [D$_6$]acetone + CF_3COOH): $\delta = 9.28$ (s, 1H), 9.21 (s, 1H), 8.98 (br s, 1H), 8.69 (br s, 1H), 4.02 (t, $J = 6$ Hz, 2H), 3.08 (t, $J = 6$ Hz, 2H), 1.79–1.49 (br m, 4H), 1.38 (br m, 8H), 0.99–0.86 (m, 6H); CH_2 and CH_3 protons adjacent to the TTF moiety were not observed; IR (KBr): $\tilde{\nu} = 2203$ (C≡N), 1742 (C=O), 1543, 1340, 1133 cm^{-1}; MS (FAB): *m*/*z* (%): 869 (27) $[M]^+$, 371 (87), 243 (100); elemental analysis calcd (%) for $C_{37}H_{35}N_5O_{10}S_5$: C 51.08, H 4.05, N 8.05; found: C 50.64, H 4.11, N 7.86.

Compound 15: Pyridine (14 μL, 0.17 mmol) followed by a solution of amine **12** (80 mg, 0.17 mmol) in dry MeCN (4 mL) were added at −30 °C to a suspension of acid chloride **5b** (80 mg, 0.17 mmol) in dry MeCN (5 mL) and the reaction mixture was stirred for 1 h at −30 °C and left to warm up to 20 °C overnight. The thick precipitate was filtered off, washed with MeCN and MeOH, and then purified by chromatography on silica gel eluting with ethyl acetate/petroleum ether (1:2 *v*/*v*) to yield compound **15** (75 mg, 55 %). M.p. 110–115 °C (decomp); ^{1}H NMR (300 MHz, [D$_6$]acetone): $\delta = 9.04$ (d, $J = 2$ Hz, 1H), 8.82 (d, $J = 2$ Hz, 1H), [*E*: 8.80 br s, *Z*: 8.75 br s (1H)], [*E*: 8.67 br s, *Z*: 8.56 br s (1H)], 7.37 (t, $J = 7$ Hz, 1H), 7.33–7.21 (m, 4H), [*Z*: 4.67 br s, *E*: 4.52 br s (2H)], [*E*: 4.29 br s, *Z*: 4.19 br s (2H)], 3.98–3.86 (m, 2H), 3.11–2.98 (m, 2H), 2.46–2.33 (m, 4H), [*E*: 1.89 br s, *Z*: 1.81 br s (3H)], 1.58–1.42 (m, 4H), 1.41–1.25 (m, 8H), 0.96–0.84 (m, 6H); ^{13}C NMR (75 MHz; [D$_6$]acetone): δ (*E*, *Z*) = 185.2, 185.0, 169.9, 169.4, 150.8, 150.7, 147.4, 147.3, 147.2, 145.3, 145.0, 138.9, 139.5, 138.2, 138.2, 137.8, 137.5, 137.4, 137.3, 131.6, 131.5, 129.7, 129.3, 128.8, 128.4, 128.2, 127.3, 126.5, 126.4, 123.3, 123.2, 52.0, 51.3, 49.2, 31.3, 28.1, 27.6, 23.0, 14.25, 14.23; some of TTF carbons are not observable; IR (KBr): $\tilde{\nu} = 1732$ (C=O), 1651, 1539, 1462, 1455, 1377, 1131, 732 cm^{-1}; MS (ES+): *m*/*z* (%): 910 (100) $[M]^+$, 911 (85) $[M+H]^+$; elemental analysis calcd (%) for $C_{41}H_{42}N_4O_{10}S_5$: C 54.05, H 4.65, N 6.15; found: C 53.78, H 4.64, N 6.01.

Compound 16: Fluorenone **15** (25 mg, 0.028 mmol) and malononitrile (25 mg, 0.38 mmol) were stirred in dry DMF (1 mL) at 20 °C for 6 h then stored at 0 °C for 12 h. The solution volume was reduced in vacuo to ca. 0.1 mL, diluted with methanol (2 mL) and the dark brown precipitate was filtered off, washed with methanol, then dissolved in CH_2Cl_2 and filtered through silica gel to give **16** (23 mg, 72 %). M.p. 137–142 °C (decomp); ^{1}H NMR (300 MHz; [D$_6$]acetone): $\delta =$ [*E*: 9.44 d, *Z*: 9.26 (d, $J = 2$ Hz, 1H)], 9.11 (br s, 1H), 8.98 (br, 1H), 8.83 (br s, 1H), 7.37 (t, $J = 7$ Hz, 1H), 7.36–7.21 (m, 4H), [*Z*: 4.77 br s, *E*: 4.49 br s (2H)], [*E*: 4.05 br m, *Z*: 3.82 br m (2H)], 3.16–3.04 (m, 2H), 1.7–1.2 (br m, 8H), 1.00–0.84 (m, 6H); CH_3 and 5 CH_2 groups closest to the TTF nucleus are not observable due to PMB; IR (KBr) $\tilde{\nu} = 2202$ (C≡N), 1653 (C=O), 1647 (C=O), 1610, 1540, 1340, 1132 cm^{-1}; MS (FAB): *m*/*z* (%): 958.2 (86) $[M]^+$, 371.2 (100); elemental analysis calcd (%) for $C_{44}H_{42}N_6O_9S_5$: C 55.10, H 4.41, N 8.76; found: C 54.91, H 4.50, N 8.39.

2,5,7-Trinitro-4-chlorocarbonylfluorene-9-one (17) was obtained as described.[13] ^{1}H NMR (200 MHz; $CDCl_3$): $\delta = 9.20$ (d, $J = 2$ Hz, 1H), 8.81 (d, $J =$ 2 Hz, 1H), 8.65 (d, $J = 2$ Hz, 1H), 8.54 (dd, $J = 8$, 2 Hz, 1H), 8.42 (d, $J =$ 8 Hz, 1H).

Compound 18: BuLi (1.6 M; 80 μL, 0.128 mmol) was added at 0 °C to a solution of compound **10** (50 mg, 0.128 mmol) in dry THF (2 mL). The reaction mixture was then cooled to −100 °C, a solution of acid chloride **17** (55 mg, 0.142 mmol) in dry THF (1.5 mL) was added dropwise and it was stirred for 1 h at −100 °C, then allowed to warm up to ca. −20 °C during 2 h and left overnight in a freezer (−15 °C). The solvent was removed in vacuo and the residue was taken up in ethyl acetate. The organic layer was subsequently washed with water, $NaHCO_3$ solution and brine, dried over $MgSO_4$ and evaporated. Flash chromatography on silica gel eluting with cyclohexane/ethyl acetate (3:1 *v*/*v*) gave a green fraction which was evaporated, the residue washed with methanol and hexane yielding **18** (70 mg, 75 %). M.p. 140 °C; ^{1}H NMR (300 MHz, [D$_6$]acetone): $\delta = 9.02$ (d, $J = 2$ Hz, 1H), 8.84 (d, $J = 2$ Hz, 1H), 8.80 (d, $J = 2$ Hz, 1H), 8.71 (d, $J =$ 2 Hz, 1H), 5.13 (s, 2H), 2.40 (m, 4H), 2.19 (s, 3H), 1.50 (m, 4H), 1.32 (m, 8H), 0.89 (m, 6H); ^{13}C NMR (75 MHz; [D$_6$]acetone, 50 °C): $\delta = 186.0$, 165.1, 150.9, 150.8, 147.4, 144.4, 140.4, 140.2, 139.4, 133.8, 132.3, 131.3, 130.0, 126.5, 123.1, 122.7, 122.4, 61.6, 32.05, 32.03, 30.2 (2C), 23.1 (2C), 14.3 (2C), 14.2; [the two central carbons of TTF were not observed (expected as low intensity peaks at 100–115 ppm), two of *C*H$_2$ carbons were hidden under the solvent signal and one signal must be overlapping with another in the aromatic region]; IR (KBr): $\tilde{\nu} = 1731$ (C=O), 1614, 1593, 1537, 1465, 1342, 1174, 739 cm^{-1}; MS (EI): *m*/*z* (%): 729 (100); elemental analysis calcd (%) for $C_{32}H_{31}N_3O_9S_4$: C 52.66, H 4.28, N 5.76; found: C 52.38, H 4.24, N 5.73. A single crystal for X-ray analysis was grown by slow cooling of an acetone solution.

 © 2002 WILEY-VCH Verlag GmbH & Co. KGaA, Weinheim 0947-6539/02/0820-4667 $ 20.00+.50/0

Compound 19: Fluorenone **18** (20 mg, 0.027 mmol) and malononitrile (12 mg, 0.18 mmol) were dissolved in DMF (0.5 mL) and stirred at 20 °C for 8 h. Then the solvent was distilled off in vacuo and the residue was triturated with methanol (1 mL). The brown precipitate was filtered off and washed with methanol giving compound **19** (20 mg, 95 %). M.p. 160 °C; ^{1}H NMR (300 MHz; [D$_6$]acetone): $\delta = 9.9 - 9.3$ (br, 2H, fluorene-*H*), 5.15 (br s, 2H), 2.40 (br s, 4H), 2.19 (br s, 3H), 1.50 (m, 4H), 1.31 (m, 8H), 0.89 (m, 6H); IR (KBr) $\tilde{\nu} = 2204$ (C≡N), 1718 (C=O), 1605, 1535, 1340 cm^{-1}; MS (FAB): *m*/*z* (%): 777 (35) $[M]^+$, 371 (100); elemental analysis calcd (%) for $C_{35}H_{31}N_5O_8S_4$: C 54.04, H 4.02, N 9.00; found: C 54.24, H 4.37, N 8.55.

2,7-Dinitro-4-chlorocarbonylfluorene-9-one (20) was obtained as described.[13] ^{1}H NMR (300 MHz; [D$_6$]acetone): $\delta = 9.11$ (d, $J = 2$ Hz, 1H), 9.04 (d, $J = 2$ Hz, 1H), 8.84 (d, $J = 2$ Hz, 1H), 8.83 (d, $J = 2$ Hz, 1H).

Compound 21: Acid chloride **20** (75 mg, 0.219 mmol) was added to a solution of TTF-CH$_2$OH (51 mg, 0.218 mmol) in dry MeCN (2 mL) resulting in the immediate precipitation of a black product. The reaction mixture was stirred overnight, the precipitate filtered off and thoroughly washed with boiling MeCN, then with acetone and methanol to give compound **21** (101 mg, 86 %). M.p. >220 °C (decomp); ^{1}H NMR (200 MHz, [D$_6$]DMSO): $\delta = 8.77$ (d, $J = 2$ Hz, 1H), 8.56 – 8.48 (m, 3H), 8.38 (d, $J = 2$ Hz, 1H), 7.07 (s, 1H), 6.71 (s, 2H), 5.31 (s, 2H); IR (KBr): $\tilde{\nu} =$ 1725 (C=O), 1609, 1587, 1523, 1451, 1343, 1267, 1223, 1155, 1087, 798, 736 cm^{-1}; MS (EI): *m*/*z* (%): 530 (8) $[M]^+$, 314 (100); elemental analysis calcd (%) for $C_{21}H_{10}N_2O_7S_4$: C 47.54, H 1.90, N 5.28; found: C 47.39, H 1.83, N 5.29.

Compound 23: Silica gel (supplied by LabPro, 0.40 g) and malononitrile (53 mg, 0.80 mmol) were added to a solution of compound **1** (108 mg, 0.30 mmol) in DMSO (1 mL) and the resulting dark-green reaction mixture was stirred at 20 °C overnight. It was then filtered from silica gel, washed with DMF and the filtrate, after evaporation in vacuo, was purified by chromatography on silica gel, eluting initially with neat ethyl acetate to remove an intermediate **22** and then with ethyl acetate/acetone (*v*/*v* 7:1) mixture. The dark-blue fraction containing **23** was collected and evaporated. The residue was dissolved in acetone (3 mL), diluted with boiling toluene (5 mL) and left to crystallize overnight in an open flask (the acetone partly evaporated). The crystalline precipitate was filtered off and washed with hot toluene affording compound **23** (40 mg, 26 %) as a potassium salt. M.p. >360 °C; ^{1}H NMR (300 MHz, [D$_6$]acetone) $\delta = 9.30$ (d, $J = 2$ Hz, 2H), 8.63 (d, $J = 2$ Hz, 2H); IR (KBr): $\tilde{\nu} = 2209$ (C≡N), 1625, 1572, 1527, 1494, 1453, 1359, 1314, 1255, 1160, 903, 829, 724 cm^{-1}; MS (ES −): *m*/*z* (%): 446 (100) $[M - K]^-$; elemental analysis calcd (%) for $C_{18}H_4KN_7O_8 \cdot H_2O$: C 42.95, H 1.20, N 19.48; found: C 42.65, H 1.35, N 19.05. A single crystal for X-ray analysis was grown from acetone solution by slow evaporation.

Salt 24: Anhydrous lithium iodide (4.0 g, 30 mmol) was added to a solution of compound **22** (200 mg, 0.495 mmol) in dry MeCN (20 mL) and the resulting dark reaction mixture was left to stand at 0 °C overnight. The precipitate was filtered in an inert atmosphere, quickly washed with cold ethyl acetate (2 mL), then with excess CH$_2$Cl$_2$ and, finally, with cold water (3 mL) to give a black powder of **24** (95 mg, 47 %). M.p. >300 °C (exothermic decomp); IR (KBr): $\tilde{\nu} = 2182$ (C≡N), 1590, 1516, 1442, 1398, 1334, 1309, 1248, 1203, 1157, 1083, 981, 827, 779, 729 cm^{-1}; MS (ES −): *m*/*z* (%): 408 (100) $[M - Li]^-$; elemental analysis calcd (%) for $C_{16}H_4LiN_6O_8 \cdot 2H_2O$: C 42.59, H 1.79, Li 1.54, N 18.63, I 0.0; found: C 42.55, H 1.33, Li 1.48, N 18.38, I 0.0.

Salt 25: A copper wire coil (diameter 0.25 mm, 99.999 %; 5 cm long) was dipped in a solution of **22** (22 mg, 0.054 mmol) in dry MeCN (4 mL) resulting in violet coloration around the wire. After two weeks at 20 °C, the reaction mixture was cooled to 0 °C, the black precipitate was scratched from the wire, filtered off, washed with ethyl acetate, and dried in vacuo (0.1 mbar, 100 °C) affording salt **25** (13 mg, 55 %). M.p. >300 °C (exothermic decomp); IR (KBr): $\tilde{\nu} =$ (cm^{-1}) 2199 (C≡N), 1593, 1526, 1438, 1410, 1334, 1313, 1245, 1211, 1155, 1077, 989, 824, 776 cm^{-1}; elemental analysis calcd (%) for $C_{16}H_4CuN_6O_8 \cdot \frac{1}{2}$MeCN: C 42.79, H 1.61, Cu 11.91, N 19.70; found: C 42.77, H 1.64, Cu 12.08, N 19.82. A single crystal for X-ray analysis was grown from MeCN solution by slow evaporation.

Acknowledgement

We thank EPSRC for funding (D.F.P.), Dr. Igor F. Perepichka (Institute of Physical Organic and Coal Chemistry, Donetsk, Ukraine) for samples of compounds **1**, **17** and **20**, Dr. David Collison (University of Manchester) for helpful discussions, and Dr. Andres E. Goeta for initial X-ray data collection for **23a**.

[1] a) J. Roncali, *Chem. Rev.* **1997**, *97*, 173 – 205; b) H. A. M. van Mullekom, J. A. J. M. Vekemans, E. W. Meijer, *Chem. Eur. J.* **1998**, *4*, 1235 – 1243; c) S. Akoudad, J. Roncali, *Chem. Commun.* **1998**, 2081 – 2082; d) C. Kitamura, K. Yoshida, Y. Yamashita, *Chem. Mater.* **1996**, *8*, 570 – 578; e) T.-T. Hung, S.-A. Chen, *Polymer* **1999**, *40*, 3881 – 3884; f) M. Kobayashi, N. Colaneri, M. Boysel, F. Wudl, A. J. Heeger, *J. Chem. Phys.* **1985**, *82*, 5717 – 5723.

[2] a) M. P. Le Paillard, A. Robert, C. Garrigou-Lagrange, P. Delhaes, P. Le Maguerès, L. Ouahab, L. Toupet, *Synth. Met.* **1993**, *58*, 223 – 232; b) V. Khodorkovsky, J. Y. Becker in *Organic Conductors. Fundamentals and Applications* (Ed.: J.-P. Farges), Marcel Dekker, New York, **1994**, pp. 75 – 113; c) Y. Yamashita, M. Tomura, *J. Mater. Chem.* **1998**, *8*, 1933 – 1944.

[3] a) P. A. Ashton, V. Balzani, J. Becher, A. Credi, M. C. T. Fyfe, G. Mattersteig, S. Menzer, M. B. Nielsen, F. M. Raymo, J. F. Stoddart, M. Venturi, D. J. Williams, *J. Am. Chem. Soc.* **1999**, *121*, 3951 – 3957; b) M. B. Nielsen, S. B. Nielsen, J. Becher, *Chem. Commun.* **1998**, 475 – 476; c) M. B. Nielsen, J. G. Hansen, J. Becher, *Eur. J. Org. Chem.* **1999**, 2807 – 2815; d) S. Fuzukumi, K. Okamoto, H. Imahori, *Angew. Chem.* **2002**, *114*, 642 – 644; *Angew. Chem. Int. Ed.* **2002**, *41*, 620 – 622.

[4] a) A. Aviram, M. Ratner, *Chem. Phys. Lett.* **1974**, *29*, 277; b) for recent discussions of this proposal see: R. M. Metzger, *J. Mater. Chem.* **1999**, *9*, 2027 – 2036; R. M. Metzger, *J. Mater. Chem.* **2000**, *10*, 55 – 62.

[5] a) M. R. Bryce, *Adv. Mater.* **1999**, *11*, 11 – 23 and references therein; b) D. M. Guldi, S. González, N. Martín, *J. Org. Chem.* **2000**, *65*, 1978 – 1983; c) N. Martín, L. Sánchez, M. A. Herranz, D. M. Guldi, *J. Phys. Chem. A* **2000**, *104*, 4648 – 4657; d) M. B. Nielsen, J. G. Hansen, J. Becher, *Eur. J. Org. Chem.* **1999**, 2807 – 2815; e) J. G. Hansen, K. S. Bang, N. Thorup, J. Becher, *Eur. J. Org. Chem.* **2000**, 2135 – 2144; f) E. Tsiperman, L. Regev, J. Y. Becker, J. Bernstein, A. Ellern, V. Khodorkovsky, A. Shames A. L. Shapiro, *Chem. Commun.* **1999**, 1125 – 1126; g) S. Sheib, M. P. Cava, J. W. Baldwin, R. M. Metzger, *J. Org. Chem.* **1998**, *63*, 1198 – 1204; h) E. Aqad, A. Ellern, L. Shapiro, V. Khodorkovsky, *Tetrahedron Lett.* **2000**, *41*, 2983 – 2986; i) M. R. Bryce, *J. Mater. Chem.* **2000**, *10*, 589 – 598; j) J. L. Segura, N. Martín, *Angew. Chem.* **2001**, *113*, 1416 – 1455; *Angew. Chem. Int. Ed.* **2001**, *40*, 1372 – 1409.

[6] a) C. A. Panetta, J. Baghdadchi, R. M. Metzger, *Mol. Cryst. Liq. Cryst.* **1984**, *107*, 103 – 113; b) C. A. Panetta, N. E. Heimer, C. L. Hussey, R. M. Metzger, *Synlett* **1991**, 301 – 309.

[7] I. F. Perepichka, L. G. Kuz'mina, D. F. Perepichka, M. R. Bryce, L. M. Goldenberg, A. F. Popov, J. A. K. Howard, *J. Org. Chem.* **1998**, *63*, 6484 – 6493 and references therein.

[8] Preliminary communication: D. F. Perepichka, M. R. Bryce, E. J. L. McInnes, J. P. Zhao, *Org. Lett.* **2001**, *3*, 1431 – 1434.

[9] D. F. Perepichka, M. R. Bryce, A. S. Batsanov, J. A. K. Howard, A. O. Cuello, M. Gray, V. M. Rotello, *J. Org. Chem.* **2001**, *66*, 4517 – 4524.

[10] I. F. Perepichka, A. F. Popov, T. V. Orekhova, M. R. Bryce, A. M. Andrievskii, A. S. Batsanov, J. A. K. Howard, N. I. Sokolov, *J. Org. Chem.* **2000**, *65*, 3053 – 3063.

[11] J.-M. Fabre, J. Garín, S. Uriel, *Tetrahedron* **1992**, *48*, 3983 – 3990.

[12] Even scratches on the glass or a polished surface of a joint could promote this side reaction, so very smooth glassware or a plastic flask is recommended to minimize the by-product formation. For the same reason, it is difficult to use TLC to monitor the reaction (excessive colorization occurs when the reaction solution is put on a silica gel or alumina TLC plate).

[13] A detailed investigation of the nucleophilic substitution in 9-dicyanomethylenepolynitrofluorenes with amines was described earlier: I. F. Perepichka, A. F. Popov, T. V. Orekhova, M. R. Bryce, A. N. Vdovichenko, A. S. Batsanov, L. M. Goldenberg, J. A. K. Howard,

 © 2002 WILEY-VCH Verlag GmbH & Co. KGaA, Weinheim 0947-6539/02/0820-4668 $ 20.00+.50/0

N. I. Sokolov, J. L. Megson, *J. Chem. Soc. Perkin Trans. 2* **1996**, 2453–2470.
[14] Elemental analysis of the silica gel (LabPro, 40/60 for chromatography) gave K, 0.64%.
[15] J. S. Chappell, A. N. Bloch, W. A. Bryden, M. Maxfield, T. O. Poehler, D. O. Cowan, *J. Am. Chem. Soc.* **1981**, *103*, 2442–2243.
[16] Unfortunately, the extremely low intensity of the CN peak in solution precludes a study of the solution IR behavior of this band.
[17] For the copper salt **25** $\tilde{\nu}_{CN}$ was somewhat higher, 2199 cm^{-1}, which is due to overlap with the peak from the solvate molecule of MeCN.
[18] V. Kampar, O. Neilands, *Russ. Chem. Rev.* **1986**, *55*, 334–342.
[19] The assignment of the protons has been made by comparison with previously investigated fluorene derivatives and on the basis of a COSY experiment (for compound **15**).
[20] For the formation of radical species from TTF in the presence of acids see: M. Giffard, P. Alonso, J. Carín, A. Gorgues, T. P. Nguyen, P. Richomme, A. Robert, J. Roncali, S. Uriel, *Adv. Mater.* **1994**, *6*, 298–300. For trialkylsubstituted TTFs the PMB was also observed in acidic solvents (e.g. $CDCl_3$).
[21] The same signal was observed for **16**.
[22] E. Ribera, C. Rovira, J. Vaciana, J. Tarrés, E. Canadell, R. Rousseau, E. Molins, M. Mas, J-P. Schoeffel, J-P. Pouget, J. Morgado, R. T. Henriques, M. Almeida, *Chem. Eur. J.* **1999**, *5*, 2025–2039.
[23] R. H. Boyd, W. D. Phillips, *J. Phys. Chem.* **1965**, *43*, 2927–2929.
[24] This is also consistent with strong EPR signal from a mixture of model D and A compounds (**6**+**7**) at high concentration (4×10^{-2} M). The intensity of this signal decreased rapidly non-linearly with lowering the concentration, and no significant signal can be observed at concentration lower then 10^{-3} M, indicating that [**6**·**11**] CTC is responsible for the EPR signal.
[25] H. M. McConnell, *J. Chem. Phys.* **1956**, *24*, 764–766.
[26] P. H. Rieger, G. K. Fraenkel, *J. Chem. Phys.* **1963**, *39*, 609–629.
[27] S. Horiuchi, H. Yamochi, G. Saito, K. Sakaguchi, M. Kusunoki, *J. Am. Chem. Soc.* **1996**, *118*, 8604–8622.
[28] J. B. Torrance, *Acc. Chem. Res.* **1979**, *12*, 79–86.
[29] M. R. Bryce, W. Devonport, A. J. Moore, *Angew. Chem.* **1994**, *106*, 1862–1864; *Angew. Chem. Int. Ed.* **1994**, *33*, 1761–1763.
[30] HOMO–LUMO gap, $\Delta E = e\ (E_{red}^{0} - E_{ox}^{0})$ eV: a) ref. [1a]; b) V. D. Parker, *J. Am. Chem. Soc.* **1976**, *98*, 98–103; c) L. E. Lyons, *Aust. J. Chem.* **1980**, *33*, 1717–1725.
[31] E.g., for **14** in CH_2Cl_2: $c = 2.90\times10^{-3}$ M, $l = 0.1$ cm, $D = 1.375 \Rightarrow \varepsilon = 4800\ M^{-1}\,cm^{-1}$; $c = 2.32\times10^{-4}$ M, $l = 1$ cm, $D = 1.143 \Rightarrow \varepsilon = 4920\ M^{-1}\,cm^{-1}$; $c = 1.66\times10^{-5}$ M, $l = 10$ cm, $D = 0.823 \Rightarrow \varepsilon = 4960\ M^{-1}\,cm^{-1}$; in CS_2: $c = 5.40\times10^{-3}$ M, $l = 0.1$ cm, D (for $\lambda_{max} = 1260$ nm) $= 2.80 \Rightarrow \varepsilon = 5190\ M^{-1}\,cm^{-1}$; $c = 1.325\times10^{-4}$ M, $l = 1$ cm, D (for $\lambda_{max} = 1231$ nm) $= 0.594 \Rightarrow \varepsilon = 4380\ M^{-1}\,cm^{-1}$; $c = 1.69\times10^{-5}$ M, $l = 10$ cm, D (for $\lambda_{max} = 1230$ nm) $= 0.714 \Rightarrow \varepsilon = 4230\ M^{-1}\,cm^{-1}$.
[32] However, the values obtained to estimate the behavior of the molecule in solution should be used with caution since the solvation energy was not taken into account.
[33] λ_{max} of these CT bands undergo the red shift as the concentration increases e.g., for **19** in CH_2Cl_2: $c = 3.34\times10^{-3}$ M, $l = 0.1$ cm, D (for $\lambda_{max} = 1325$ nm) $= 0.786 \Rightarrow \varepsilon' = 2350\ M^{-1}\,cm^{-1}$; $c = 3.34\times10^{-4}$ M, $l = 1$ cm, D (for $\lambda_{max} = 1212$ nm) $= 0.0647 \Rightarrow \varepsilon' = 190\ M^{-1}\,cm^{-1}$; ($\varepsilon'$ was determined in supposition of the intramolecular absorption).
[34] a) R. J. Mortimer, *Chem. Soc. Rev.* **1997**, *26*, 147–156; b) S. Hünig, M. Kemmer, H. Wenner, I. F. Perepichka, P. Bäuerle, A. Emge, G. Gescheit, *Chem. Eur. J.* **1999**, *5*, 1969–1973; c) D. R. Rosseinsky, R. J. Mortimer, *Adv. Mater.* **2001**, *13*, 783–793.
[35] M. Mastragostino, in *Electrochromic Devices* (Ed.: B. Scrosati), Chapman & Hall, London **1993**, Chapter 7, pp. 223–249.
[36] Appearance of the same bands was observed by electrochemical oxidation of TTF derivative **11** (Figure S7).
[37] The assignment of these bands is supported by spectroelectrochemical experiments on the fluorene derivative **6** (Figure S8) and the electronic spectra of isolated fluorene ion-radical salt **24**.
[38] J. Silverman, N. F. Yannoni, A. P. Krukonis, *Acta Crystallogr. Sect. B* **1974**, *30*, 1474–1480.
[39] A. S. Batsanov, I. F. Perepichka, M. R. Bryce, J. A. K. Howard, *Acta Crystallogr. Sect. C* **2001**, *57*, 1299–1302.
[40] a) W. Flandrois, D. Chasseau, *Acta Crystallogr. Sect. B* **1977**, *33*, 2744–2750; b) T. J. Kistenmacher, T. J. Emge, A. N. Bloch, D. O. Cowan, *Acta Crystallogr. Sect. B* **1982**, *38*, 1193–1199; c) A. S. Batsanov, M. R. Bryce, A. Chesney, J. A. K. Howard, D. E. John, A. J. Moore, C. L. Wood, H. Gershtenman, J. Y. Becker, V. Y. Khodorkovsky, A. Ellern, J. Bernstein, I. F. Perepichka, V. Rotello, M. Gray, A. O. Cuello, *J. Mater. Chem.* **2001**, *11*, 2181–2191.
[41] R. A. Heintz, H, Zhao, X. Ouyang, G. Gandinetti, J. Cowen, K. R. Dunbar, *Inorg. Chem.* **1999**, *38*, 144–156.
[42] J. J. Stezowski, *Acta Crystallogr. Sect. B* **1977**, *33*, 2472–2476.
[43] V. N. Nesterov, V. E. Shklover, Yu. T. Struchkov, Yu. A. Sharanin, A. I. Aitov, A. M. Shestopalov, *Acta Crystallogr. Sect. C* **1991**, *47*, 109–112.
[44] C. M. Duff, G. A. Heath, *Inorg. Chem.* **1991**, *30*, 2528–2535.
[45] *SHELXTL*, Version 5.1, Bruker AXS Inc., Madison, Wisconsin, USA, **1998**.
[46] D. F. Perepichka, M. R. Bryce, I. F. Perepichka, S. B. Lyubchik, C. A. Christensen, N. Godbert, A. S. Batsanov, E. Levillain, E. J. L. McInnes, J. P. Zhao, *J. Am. Chem. Soc.* in press.
[47] The yield could possibly be improved by using 5–10 times lower concentration.

Received: April 9, 2002 [F4009]